

# Efficient Backdoor Attacks for Deep Neural Networks in Real-world Scenarios

Hong Sun<sup>1,\*</sup> Ziqiang Li<sup>1,\*</sup> Pengfei Xia<sup>1</sup> Heng Li<sup>2</sup> Beihao Xia<sup>2</sup> Yi Wu<sup>1</sup> Bin Li<sup>1</sup>

<sup>1</sup>Big Data and Decision Lab, University of Science and Technology of China.

<sup>2</sup>Huazhong University of Science and Technology

{hsun777, iceli, xpengfei}@mail.ustc.edu.cn, {liheng, xbh\_hust}@hust.edu.cn

wuyi2021@mail.ustc.edu.cn, binli@ustc.edu.cn

## Abstract

Recent deep neural networks (DNNs) have come to rely on vast amounts of training data, providing an opportunity for malicious attackers to exploit and contaminate the data to carry out backdoor attacks. These attacks significantly undermine the reliability of DNNs. However, existing backdoor attack methods make unrealistic assumptions, assuming that all training data comes from a single source and that attackers have full access to the training data. In this paper, we address this limitation by introducing a more realistic attack scenario where victims collect data from multiple sources, and attackers cannot access the complete training data. We refer to this scenario as **data-constrained backdoor attacks**. In such cases, previous attack methods suffer from severe efficiency degradation due to the **entanglement** between benign and poisoning features during the backdoor injection process.

To tackle this problem, we propose a novel approach that leverages the pre-trained Contrastive Language-Image Pre-Training (CLIP) model. We introduce three CLIP-based technologies from two distinct streams: *Clean Feature Suppression*, which aims to suppress the influence of clean features to enhance the prominence of poisoning features, and *Poisoning Feature Augmentation*, which focuses on augmenting the presence and impact of poisoning features to effectively manipulate the model's behavior.

To evaluate the effectiveness, harmlessness to benign accuracy, and stealthiness of our method, we conduct extensive experiments on 3 target models, 3 datasets, and over 15 different settings. The results demonstrate remarkable improvements, with some settings achieving over **100%** improvement compared to existing attacks in data-constrained scenarios. Our research contributes to addressing the limitations of existing methods and provides a practical and effective solution for data-constrained backdoor attacks.

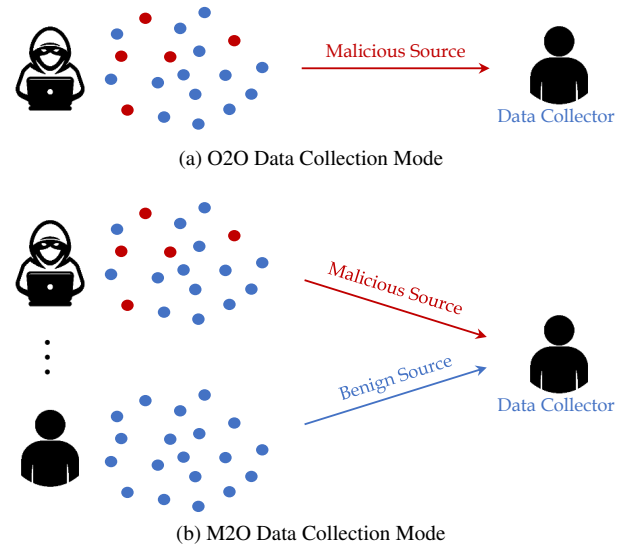


Figure 1: One-to-one (O2O) and many-to-one (M2O) data collection modes. M2O mode is more in line with practical scenarios where data collectors collect data from multiple sources. In this mode, the attacker cannot have all the data available to the victims.

## 1 Introduction

Deep neural networks (DNNs) are widely utilized and powerful machine learning algorithms inspired by the structure and functioning of the human brain. They excel at learning intricate patterns in data, making them invaluable for various applications such as image recognition [17, 21], natural language processing [33, 68], image generation [20, 30], and anomaly detection [45, 64]. However, the effectiveness of DNNs heavily relies on the quantity and quality of the training data. For instance, Stable Diffusion [49], a generative model with 983 million parameters, owes its success in image generation tasks to pre-training on 5 billion image-text pairs. Similarly, GPT-3 [3], a language model with 175 billion

\*Equal Contribution.

parameters, owes its efficacy in diverse language processing tasks to pre-training on an extensive corpus of 45 TB of text data. As the demand for data continues to rise, many users and businesses resort to third-party sources or online collections as a convenient means of acquiring the necessary data. However, recent studies [2, 15, 18, 25, 43, 64] have demonstrated that such practices can be maliciously exploited by attackers to contaminate the training data, significantly impairing the functionality and reliability of trained models.

The growing adoption of neural networks across different domains has made them an attractive target for malicious attacks. One particular attack technique gaining attention is the *backdoor attack* [2, 9, 15, 24, 26, 27, 41]. In backdoor attacks, a neural network is deliberately injected with a hidden trigger by introducing a small number of poisoning samples into the benign training set during the training. Once the model is deployed, the attacker can activate the backdoor by providing specific inputs containing the hidden trigger, causing the model to produce incorrect results. Backdoor attacks continue to present a significant and pervasive threat across multiple sectors, including image classification [16], natural language processing [43], speaker verification [67], malware detection [24], and video recognition [69]. In this paper, we focus on the widely studied field of image classification.

However, it is important to note that all of previous backdoor attacks are based on an assumption that may be too broad in practice. They assume that all training data has been collected from a single source, and the collected source has been poisoned by attacker (As depicted in the O2O data collection mode in Fig. 1). In this case, the attacker can full access to the entire training data. While this assumption allows attackers to easily poison the training data, it does not accurately reflect real-world attack scenarios. To illustrate this point, let’s consider a scenario where victims possess a private dataset with limited samples. To compensate for the limited data, victims may need to augment their dataset by collecting additional data from multiple sources on the internet (referred to as the public dataset) and combine it with their private dataset to form the training set. As shown in the M2O data collection mode in Fig. 1, part of the sources may be poisoned by attackers, secretly\*. In this case, the attackers cannot access the private dataset and can only manipulate a portion of the public dataset to carry out the poisoning process. Consequently, a discrepancy arises between the distribution of the poisoning data and the distribution of the training data, which differs from the previous pipeline of poisoning attacks.

In this paper, we address a more realistic backdoor attack scenario called **data-constrained backdoor attacks**, where the attackers do not have access to the entire train-

ing set. To be more precise, we classify data-constrained backdoor attacks into three types based on different types of data sources: number-constrained backdoor attacks, class-constrained backdoor attacks, and domain-constrained backdoor attacks<sup>†</sup>. Upon investigation, we have discovered that existing attack methods exhibit significant performance degradation when dealing with these data-constrained backdoor attacks. We propose that the **entanglement** between benign and poisoning features is a crucial factor contributing to this phenomenon. Entanglement refers to the neural networks utilizing both benign and poisoning features to make decisions for poisoning samples. However, this approach is not efficient for backdoor attacks. Ideally, an efficient backdoor attack should solely rely on the poison feature generated by the trigger to make decisions, irrespective of how the benign feature is expressed.

To address the aforementioned challenge and enhance the efficiency of poisoning attacks in data-constrained backdoor scenarios, we introduce two streams: *Clean Feature Suppression* and *Poisoning Feature Augmentation*. In the Clean Feature Suppression stream, we focus on reducing the influence of clean features during the poisoning process. On the other hand, in the Poisoning Feature Augmentation stream, we aim to amplify the expression of poisoning features. To achieve these goals, we propose three techniques utilizing the pre-trained Contrastive Language-Image Pre-Training (CLIP) [46] model.

i) *CLIP-based Clean Feature Erasing (CLIP-CFE)* is designed to suppress the expression of clean features. It leverages the capabilities of the CLIP model to identify and minimize the impact of clean features in the poisoning process.

ii) *CLIP-based Universal Adversarial Perturbations (CLIP-UAP)* focuses on poisoning feature augmentation. It employs the CLIP model to generate universal adversarial perturbations that effectively enhance the expression of poisoning features in the training data.

iii) *CLIP-based Contrastive Feature Augmentation (CLIP-CFA)* also falls under the poisoning feature augmentation stream. This technique utilizes the CLIP model to perform contrastive feature augmentation, enhancing the power of poisoning features and improving the effectiveness of the backdoor attack.

Our main contributions are summarized as follows.

- We present a novel and contemporary backdoor attack scenario called data-constrained backdoor attacks to image classification. Data-constrained backdoor attacks assume that attackers lack access to the entire training data, making it a versatile and practical attack with broad

\*This scenario is common in the context of large models training. For instance, Stable Diffusion [49], a popular generative model, pre-trains on 5 billion image-text pairs. Similarly, GPT-3 [3], a language model with 175 billion parameters, pre-trains on an extensive corpus of 45 TB of text data. Both of them need to crawl large amounts of data from different websites to complete complex training tasks.

<sup>†</sup>These three backdoor attacks are more realistic attack scenario, where the data provided by each data source is independently and identically distribution in number-constrained backdoor attacks, each data source provides data belonging to different categories in class-constrained backdoor attacks, and each data source provides data from different domains in domain-constrained backdoor attacks. More description can be found in Sec. 3.

applicability.

- Through a systematic analysis of previous attack methods, we identify the entanglement between poisoning and benign features as the primary contributing factor to their performance degradation.
- To address this issue, we introduce the pre-trained CLIP model into the field of backdoor attacks for the first time. We propose three innovative technologies: CLIP-CFE, CLIP-UAP, and CLIP-CFA. Extensive evaluations conducted on 3 datasets and 3 target models, and over **15** different settings demonstrate the significant superiority of our proposed CLIP-UAP and CLIP-CFA over existing backdoor attacks. Furthermore, CLIP-CFE complements existing attack methods and can be seamlessly integrated with them, resulting in further efficiency improvements.

## 2 Background

Here we first summary the common pipeline of backdoor attacks on neural networks, and then we introduce the Contrastive Language-Image Pre-Training (CLIP) Model that has been adopted in our method.

### 2.1 Backdoor Attacks on Neural Networks

#### 2.1.1 General Pipeline of Backdoor Attacks

Consider a learning model  $f(\cdot; \Theta) : X \rightarrow Y$ , where  $\Theta$  represents the model's parameters and  $X(Y)$  denotes the input (output) space, with given dataset  $\mathcal{D} \subset X \times Y$ . Backdoor attacks typically involve three essential steps: *poisoning set generation*, *backdoor injection*, and *backdoor activation*.

**Poisoning set generation.** In this step, attackers employ a pre-defined poison generator  $\mathcal{T}(x, t)$  to introduce a trigger  $t$  into a clean sample  $x$ . Specifically, they select a subset  $\mathcal{P}' = \{(x_i, y_i) | i = 1, \dots, P\}$  from the clean training set  $\mathcal{D} = \{(x_i, y_i) | i = 1, \dots, N\}$  ( $\mathcal{P}' \subset \mathcal{D}$ , and  $P \ll N$ ) and result in the corresponding poisoning set  $\mathcal{P} = \{(x'_i, k) | x'_i = \mathcal{T}(x_i, t), (x_i, y_i) \in \mathcal{P}', i = 1, \dots, P\}$ . Here,  $y_i$  and  $k$  represent the true label and the attack-target label of the clean sample  $x_i$  and the poisoning sample  $x'_i$ , respectively.

**Backdoor injection.** In this step, The attackers mix the poisoning set  $\mathcal{P}$  into the clean training set  $\mathcal{D}$  and release the new dataset. The victims download the poisoning dataset and use it to train their own DNN models [16]:

$$\min_{\Theta} \frac{1}{N} \sum_{(x, y) \in \mathcal{D}} L(f(x; \Theta), y) + \frac{1}{P} \sum_{(x', k) \in \mathcal{P}} L(f(x'; \Theta), k), \quad (1)$$

where  $L$  is the classification loss such as the commonly used cross entropy loss. In this case, backdoor injection into DNNs has been completed silently.

**Backdoor activation.** In this step, the victims deploy their compromised DNN models on model-sharing platforms and

model-selling platforms, such as Model Zoo and AWS Marketplace. The compromised model behaves normally when presented with benign inputs, but attackers can manipulate its predictions to align with their malicious objectives by providing specific samples containing pre-defined triggers.

#### 2.1.2 Examples of Backdoor Attacks

Here, we present three popular backdoor attack methods that serve as the baseline for our preliminary experiments, providing insight into the motivation discussed in Sec. 3. All attacks follow the pipeline described in Sec. 2.1.1.

**BadNets [16].** BadNets [16] is the pioneering backdoor attack in deep learning and is often used as a benchmark for subsequent research. It utilizes a  $2 \times 2$  attacker-specified pixel patch as the universal trigger pattern attached to benign samples.

**Blended [5]** Chen *et al.* [5] first discuss the requirement for invisibility in backdoor attacks. They propose that the poisoning image should be visually indistinguishable from its benign counterpart to evade human inspection. To meet this requirement, they introduce a blending strategy where poisoning images are created by blending the backdoor trigger with benign images. Formally, the poison generator can be formulated as  $\mathcal{T}(x, t) = \lambda \cdot t + (1 - \lambda) \cdot x$ , where  $\lambda$  represents the blend ratio (we set  $\lambda = 0.15$  for all experiments in this paper), and  $t$  is an attacker-specified benign image serving as the universal trigger pattern.

**Universal Adversarial Perturbations (UAP) [70]** Inspired by Universal Adversarial Perturbations (UAPs) in adversarial examples, some studies [9, 26, 70] propose optimizing a UAP on a pre-trained clean model as the natural trigger, formulated as  $\mathcal{T}(x, t) = x + t$ , where  $t$  is a pre-defined UAP serving as the universal trigger pattern. It's worth noting that UAP-based backdoor attacks require a clean model pre-trained on the entire training set, which is not suitable for the discussed settings. However, to better explain our motivation that previous technologies exhibit significant performance degradation in data-constrained backdoor attacks, we assume the availability of a clean model pre-trained on the original training dataset in this section. It is important to acknowledge that this assumption does not hold in an actual attack scenario.

### 2.2 Contrastive Language-Image Pre-Training (CLIP) Model

Our method introduces the Contrastive Language-Image Pre-Training (CLIP) [46] model into backdoor injection and we introduce it here. CLIP is a revolutionary deep learning model developed by OpenAI that is designed to connects texts and images by bringing them closer in a shared latent space, under a contrastive learning manner. The CLIP model is pre-trained on 400 million image-text pairs harvested from the Web, containing two encoder: CLIP text encoder  $\hat{\mathcal{E}}_t(\cdot)$  and CLIP image encoder  $\hat{\mathcal{E}}_i(\cdot)$ . These encoders project the text and image to

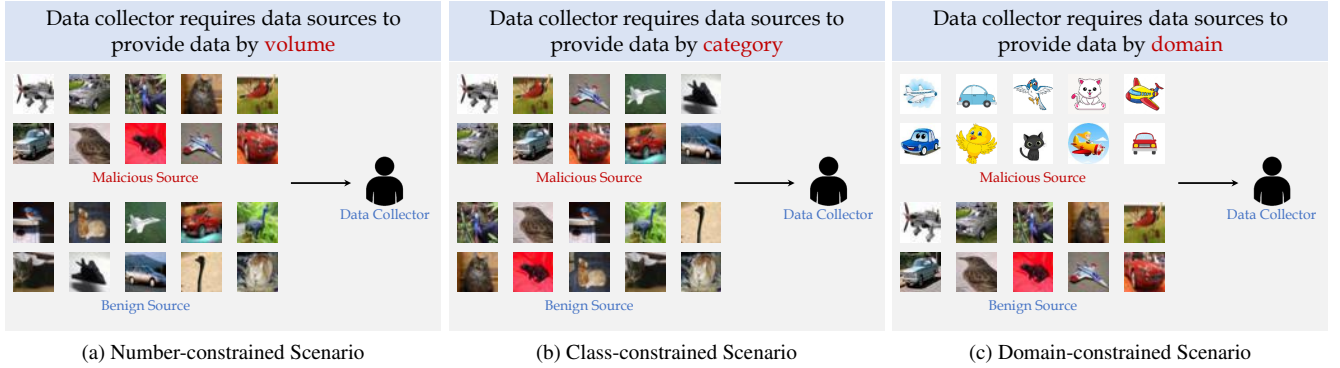


Figure 2: Three data-constrained attack scenarios, where the data provided by each data source is independently and identically distribution in number-constrained backdoor attacks, each data source provides data belonging to different categories in class-constrained backdoor attacks, and each data source provides data from different domains in domain-constrained backdoor attacks.

the CLIP common embedded feature space. Since natural language is able to express a much wider set of visual concepts, it contains ability to generalize across a wide range of tasks and domains, such as text-driven image manipulation [44], zero-shot classification [6], domain generalization [42]. To our best knowledge, our paper is the first study to explore the usage of CLIP model in the security community.

### 3 Data-constrained Backdoor Attacks

Here we first show the considered pipeline of data-constrained backdoor attacks, and then illustrate the performance degradation of previous attack methods on proposed data-constrained backdoor attacks. Finally, we attribute the degradation to the entanglement between the benign and poisoning features during the poisoning injection.

#### 3.1 Preliminaries

Previous methods [5, 12, 16, 27, 34, 39, 41, 59, 60] have commonly followed the attack pipeline outlined in Sec. 2.1.1. However, this widely adopted pipeline relies on an overly loose assumption that all training data is collected from a single source and that the attacker has access to the entire training data, which is often not the case in real-world attack scenarios. In this paper, we focus on a more realistic scenario: *Data-constrained Backdoor Attacks*, which necessitates the definition of a modified attack pipeline as follows:

**Pipeline of data-constrained backdoor attacks.** Similar to the general pipeline of backdoor attacks on neural networks, the proposed pipeline also consists of three steps: *poisoning set generation*, *backdoor injection*, and *backdoor activation*. The backdoor injection and activation steps remain unchanged from the previous pipeline. However, in the poisoning set generation step, data-constrained backdoor attacks differ from the previous pipeline. Instead of assuming access to the entire dataset  $\mathcal{D}$ , data-constrained attacks only assume access to a

clean training set  $\mathcal{D}' = \{(x_i, y_i) | i = 1, \dots, N'\}$ , which follows a different data distribution from  $\mathcal{D}$ . To address this, the attacker randomly selects a subset  $\mathcal{P}' = \{(x_i, y_i) | i = 1, \dots, P\}$  from the accessible dataset  $\mathcal{D}'$ , and creates the corresponding poisoning set  $\mathcal{P} = \{(x'_i, k) | x'_i = \mathcal{T}(x_i, t), (x_i, y_i) \in \mathcal{P}', i = 1, \dots, P\}$ . Additionally, based on the different constraints imposed by the accessible training set  $\mathcal{D}'$ , data-constrained backdoor attacks are further categorized into three types: *Number-constrained Backdoor Attacks*, *Class-constrained Backdoor Attacks*, and *Domain-constrained Backdoor Attacks*. The details can be found in Sec. 3.2, Sec 3.3, and Sec. 3.4, respectively.

**Experimental settings.** To evaluate the performance of three backdoor attack methods (BadNets, Blended, and UAP) under data-constrained scenarios, we conduct experiments on the CIFAR-10 dataset. Specifically, we consider three types of data constraints: number, class, and domain. The settings for the poisoning attacks follow those described in Sec. 2.1.2. In all attacks, we set the attack-target label  $k$  to category 0. For our experiments, we select the VGG-16 model as the victim model and employ SGD as the optimizer with a weight decay of  $5e-4$  and a momentum of 0.9. The batch size is set to 256, and the initial learning rate is set to 0.01. The learning rate is multiplied by 0.1 at the 35-th and 55-th epochs, and the training is conducted for a total of 70 epochs.

#### 3.2 Number-constrained Backdoor Attacks

**Definition.** Let  $\mathcal{D}'$  denote the data manipulable by the malicious source, and  $\mathcal{D}$  represent all the data available to the data collector. In the number-constrained scenario, as illustrated in Fig. 2 (a), the data collector gathers data from multiple sources, including both malicious and benign sources, to form  $\mathcal{D}$ . The data provided by each data source is independently and identically distributed. In other words,  $\mathcal{D}$  and  $\mathcal{D}'$  belong to the same distribution, but in terms of quantity,  $N' < N$ . The setting of number-constrained backdoor attacks is similar to that of data-efficient backdoor attacks discussed in previous



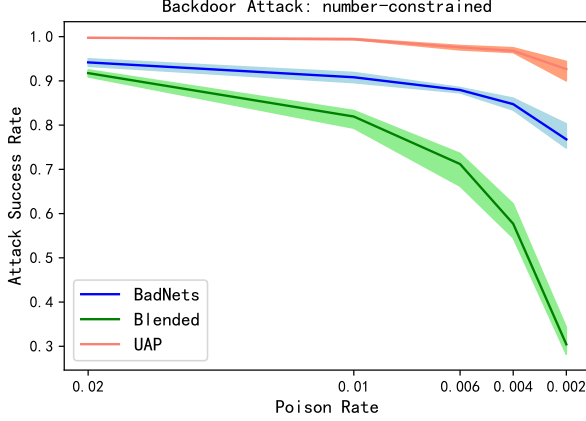


Figure 3: The attack success rate (ASR) in the number-constrained backdoor attacks. The abscissa is the number ( $P$ ) of samples in the poisoning set  $\mathcal{P}'$ . The experiment is repeated 5 times, and the solid lines represent the mean results.

studies [60, 70]. Both aim to improve the Attack Success Rate (ASR) under a low poisoning rate. However, previous studies assumed that the attacker has access to the entire training set  $\mathcal{D}$ , which enables efficient trigger design and sample selection. For example, some studies [70] draw inspiration from Universal Adversarial Perturbations (UAPs) in adversarial examples and propose to optimize a UAP on a clean model pre-trained on the training set as the natural trigger. Xia *et al.* [60] enhance the poisoning efficiency in backdoor attacks by selecting poisoning data from the entire training set. Although these methods have achieved remarkable results, they cannot be directly applied to number-constrained backdoor attacks due to the lack of access to the entire training set.

**Experimental results.** In this section, we investigate the performance degradation of previous studies in number-constrained backdoor attacks. As shown in Fig. 3, the attack success rate experiences a significant decrease as the number ( $P$ ) of poisoning samples decreases, particularly for Blended backdoor attacks. It is worth noting that Universal Adversarial Perturbations (UAP) achieves relatively favorable results even with a low poisoning rate. This can be attributed to the utilization of a proxy model that is pre-trained on the entire training set ( $\mathcal{D}$ ). However, in our settings, UAP is not accessible, and we present the results for UAP to effectively demonstrate the performance degradation even when a pre-trained proxy model is available.

### 3.3 Class-constrained Backdoor Attacks

**Definition.** In the class-constrained scenario, let  $\mathcal{D}'$  represent the data manipulable by the malicious source, and  $\mathcal{D}$  denote all the data available to the data collector. As depicted in part (b) of Fig. 2, the data collector gathers data from multiple sources, including both malicious and benign sources, to form  $\mathcal{D}$ . Each data source provides data belonging to dif-

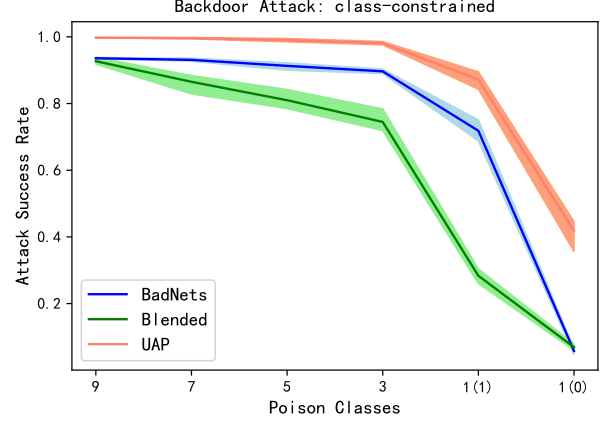


Figure 4: The attack success rate (ASR) in the class-constrained backdoor attack. The experiments are conducted with triggers BadNets, Blended, and UAP, with a poisoning rate of 2% ( $P = 1000$ ) for each. The x-axis represents the number of classes ( $|Y'|$ ) in the poisoning set  $\mathcal{P}'$ . Specifically, '1 (1)' and '1 (0)' denote dirty-label single-class ( $Y' = \{c\}, c \neq k$ ) and clean-label single-class ( $Y' = \{k\}$ ), respectively. The experiment is repeated 5 times, and the solid lines indicate the average results.

ferent categories, resulting in  $\mathcal{D}'$  containing only a subset of categories present in  $\mathcal{D}$ . Therefore,  $\mathcal{D}$  and  $\mathcal{D}'$  follow distinct distributions. More specifically, the accessible clean training set  $\mathcal{D}' \subset X \times Y'$  ( $\mathcal{D}' = \{(x_i, y_i) | i = 1, \dots, N'\}$ ) is a subset of the entire training set  $\mathcal{D} \subset X \times Y$  ( $\mathcal{D} = \{(x_i, y_i) | i = 1, \dots, N\}$ ), where  $Y' \subset Y = \{1, 2, \dots, C\}$ . Class-constrained backdoor attacks can be seen as a general setting of clean-label backdoor attacks [50, 53, 54]. In clean-label backdoor attacks, the accessible clean training set  $\mathcal{D}'$  is defined as  $\mathcal{D}' \subset X \times Y'$ , where  $Y' = \{k\}$  and  $k$  represents the attack-target label.

**Experimental results.** In this section, we explore the performance degeneration of previous studies in class-constrained backdoor attacks. As illustrated in Fig. 4, attack success rate decreases as the number of class ( $C'$ ) in the poisoning set decreases, which is the similar as experimental results on the number-constrained backdoor attacks.

### 3.4 Domain-constrained Backdoor Attacks

**Definition.** In the domain-constrained scenario, as depicted in part (c) of Fig. 2, the data collector gathers data from multiple sources (both malicious and benign) to form  $\mathcal{D}$ . Each data source provides data from a different domain, resulting in  $\mathcal{D}'$  containing only a subset of the domains present in  $\mathcal{D}$ . Consequently,  $\mathcal{D}$  and  $\mathcal{D}'$  belong to different distributions. We examine an extreme scenario in domain-constrained backdoor attacks, where the test dataset follows the same distribution as the benign source ( $\mathcal{D} \setminus \mathcal{D}'$ ) and is outside the domain of the malicious source  $\mathcal{D}' \subset X \times Y'$  ( $\mathcal{D}' = \{(x_i, y_i) | i = 1, \dots, N'\}$ ).

**Experimental results.** To simulate the domain-constrained

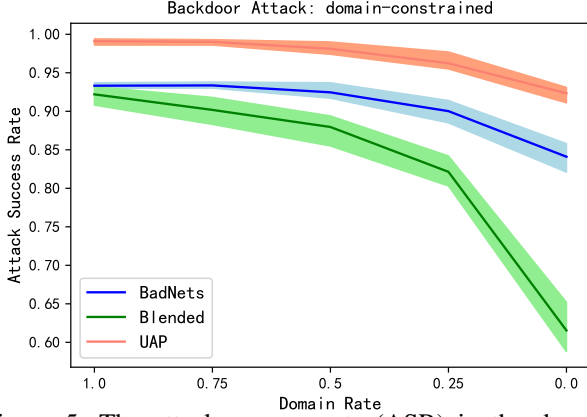


Figure 5: The attack success rate (ASR) in the domain-constrained backdoor attack. The poisoning rates of experiments with trigger BadNets, Blended, and UAP are 2% ( $P = 1000$ ), 2% ( $P = 1000$ ), and 1% ( $P = 500$ ), respectively. The abscissa is the domain rate that represents the proportion of poisoning sets sampled from  $\mathcal{D} \setminus \mathcal{D}'$  and  $\mathcal{D}'$ . The experiment is repeated 5 times, and the solid lines represent the mean runs.

scenario, we conducted experiments with the following settings in this section: we designate the CIFAR-10 dataset as the benign source, the ImageNet dataset as the malicious source, and evaluated the attack performance on the CIFAR-10 dataset. Fig. 5 illustrates the results, showing a decrease in the attack success rate as the domain rate (the proportion of poisoning sets sampled from  $\mathcal{D} \setminus \mathcal{D}'$  and  $\mathcal{D}'$ ) in the poisoning set decreases. This observation aligns with the experimental findings in the number-constrained and class-constrained backdoor attacks.

### 3.5 Entanglement Between Benign and Poisoning Features

In our data-constrained backdoor attacks, we have made two significant observations. Firstly, we have noticed a severe performance decline in class-constrained and domain-constrained backdoor attacks. Secondly, we consistently found that BadNets outperforms Blended in terms of attack efficiency. We attribute these observations to the entanglement between benign and poisoning features. Our study is the first to investigate feature entanglement in the context of backdoor attacks, providing new insights into backdoor learning. Ideally, we would expect backdoor models to rely solely on poisoning features to make decisions when encountering poisoning samples, as this would be the most efficient approach for backdoor attacks. However, neural networks tend to be greedy and utilize all features for decision-making [31], leading to activation of both poisoning and benign features during backdoor injection. This results in reduced poisoning efficiency when there is a difference in benign features between the backdoor injection and activation phases, as observed in

data-constrained backdoor attacks.

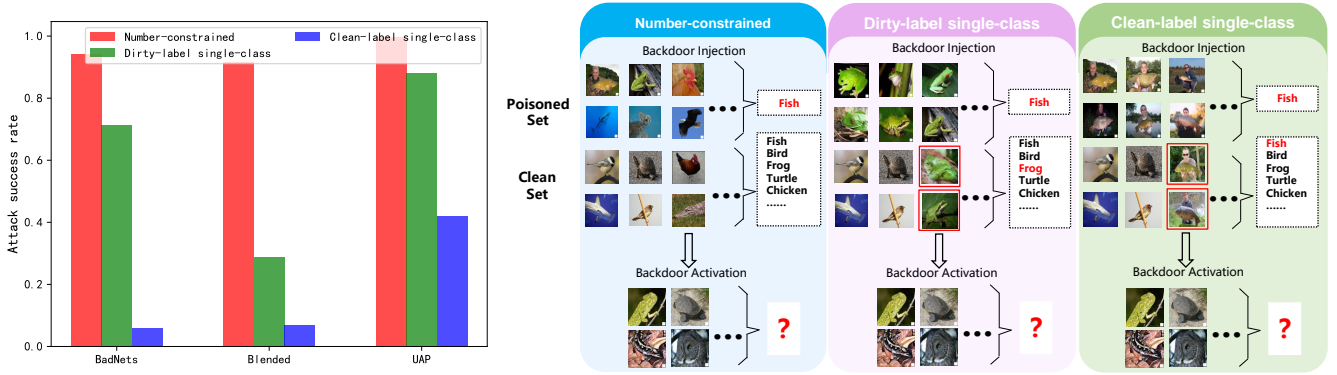
We have further investigated our hypothesis and present our findings in Fig. 6. As shown in Fig. 6 (a), the attack efficiency of number-constrained, dirty-label single-class, and clean-label single-class backdoor attacks<sup>‡</sup> decreases in turn under the same poison rate. To understand the reason behind this phenomenon, we provide visualizations of the backdoor injection and activation phases for these three attacks in Fig. 6 (b). For the **number-constrained backdoor attack**, the distribution of poisoning samples (consisting of both benign and poisoning features) in the backdoor injection phase is the same as that in the backdoor activation phase. In other words, both benign and poisoning features are activated simultaneously during both phases. However, for the **dirty-label single-class backdoor attack**, the distribution of poisoning samples (consisting of single-class benign and poisoning features) in the backdoor injection phase is different from that in the backdoor activation phase. During the injection phase, both benign and poisoning features are activated, but during activation phase, only the poisoning feature is activated. This is the reason why previous attack methods on dirty-label single-class backdoor attacks exhibit performance degeneration. The **clean-label single-class backdoor attack** is similar to the dirty-label single-class backdoor attack in terms of the distribution of poisoning samples. However, during backdoor injection, there is competing activation<sup>‡</sup> between benign and poisoning features. Consequently, the poisoning efficiency of clean-label single-class backdoor attacks is lower than that of dirty-label single-class backdoor attacks.

In summary, performance degeneration in data-constrained backdoor attacks can be attributed to entanglement between benign and poisoning features. BadNets exhibits simpler triggers compared to Blended, leading to less entanglement and a higher attack success rate.

## 4 CLIP-guided Backdoor Attacks Method

In this section, we present our approach, which consists of two components: **Clean Feature Suppression** and **Poisoning Feature Augmentation**. These components are independent of each other and can be seamlessly combined. Specifically, Clean Feature Suppression can be implemented through *CLIP-based Clean Feature Erasing (CLIP-CFE)*, and Poisoning Feature Augmentation has included two technolo-

<sup>‡</sup>In the clean-label single-class backdoor attack, the benign feature of the accessible class (the same as the attack-target class) in both poisoning and clean sets is labeled with the same label (e.g., "Fish" in Fig. 6), and the clean set contains more samples of the attack-target class. As a result, the presence of the benign feature in the poisoning set hampers the activation of the poisoning features. In contrary, the benign feature of the accessible class in poisoning and clean sets is labeled with the different label in the dirty-label single-class backdoor attack (e.g., the benign feature in the clean set is labeled as "Frog", while the benign+poisoning feature in the poisoning set is labeled as "Fish"). Consequently, the benign feature in the poisoning set does not impact the activation of the poisoning features.



(a) ASR of three backdoor attacks under the same poisoning rate ( $p = 1000$ ) on the CIFAR-10 dataset. (b) Visualizations of the backdoor injection and activation phases for three backdoor attacks.

Figure 6: Analyses the entanglement between benign and poisoning features on the number-constrained, dirty-label single-class, and clean-label single-class backdoor attacks.

gies: *CLIP-based Universal Adversarial Perturbations (CLIP-UAP)* and *CLIP-based Contrastive Feature Augmentation (CLIP-CFA)*. By seamlessly integrating these two orthogonal aspects, our method presents a comprehensive and versatile solution that addresses all three types of data-constrained backdoor attacks. Before proposing the attack method, we first introduce threat model considered in our work.

## 4.1 Threat Model

**Attack scenario.** The proliferation of large-scale artificial intelligence models, such as ChatGPT and Stable Diffusion, necessitates the collection of massive amounts of data from the web. However, the security and trustworthiness of this data cannot always be guaranteed. This data collection pipeline inadvertently introduces vulnerabilities that can be exploited by data-based backdoor attacks. Attackers can strategically inject poisoning data into the training dataset and publish it on the internet, potentially compromising the integrity and performance of these models. Unlike previous attack scenarios where all training data is sourced from a single provider, we consider a more realistic scenario in which victims collect data from multiple sources. In this scenario, attackers only have access to a portion of the training dataset. This situation mirrors the real-world training process of models that utilize diverse public data. By acknowledging the challenges posed by multi-source data collection and limited attacker access, our study provides valuable insights into the security implications of such scenarios.

**Attack goal.** The objective of our paper is aligned with popular backdoor attacks, as seen in previous studies [16, 24]. The attackers aim to activate a hidden trigger within the model by providing specific inputs, leading the model to produce incorrect results. Our attack strategy emphasizes three key properties: (i) *Minimal side effects*: The backdoor attacks should not adversely impact the accuracy of the model on

benign inputs. (ii) *Effective backdoor*: The attack should have a high success rate across various datasets and models, ensuring its efficiency. (iii) *Stealthy attack*: The backdoor attacks should be inconspicuous and difficult to detect, maintaining their stealthiness. Our research aims to develop invigorative backdoor attacks that strike a balance between effectiveness and preserving the integrity of the model’s performance on legitimate inputs.

**Attackers’ prior knowledge.** In order to simulate a realistic scenario, we assume that the attackers have no access to the models or training details. They possess only general knowledge about the class labels involved in the task. This assumption reflects a more challenging and practical setting, where attackers have limited information about the target system.

**Attackers’ capabilities.** Building upon previous studies [16], we make the assumption that the attackers possess the capability to control the training data. However, we further impose a stricter assumption in this work, stating that the attackers have control over only a portion of the training data. Consequently, we divide the attack scenario into three distinct tasks, each representing different capabilities of the attacker. These tasks include: (i) *Number-constrained backdoor attacks*, where the attacker has access to only a subset of the training data; (ii) *Class-constrained backdoor attacks*, where the attacker has access to only a subset of the classes in the training data; and (iii) *Domain-constrained backdoor attacks*, where the attacker has access to only a subset of the domains within the training data. By considering these various constraints, we provide a comprehensive analysis of backdoor attacks in different data-constrained scenarios.

## 4.2 Clean Feature Suppression

As described in Sec. 3, the effectiveness of data-constrained backdoor attacks is hindered due to the entanglement of be-

nign and poisoning features during the backdoor injection phase. To address this challenge, we propose a solution called "clean feature suppression" in this section. The primary objective of this approach is to minimize the impact of benign features on the decision-making process, thus amplifying the significance of poisoning features.

#### 4.2.1 CLIP-based Clean Feature Erasing

To achieve clean feature suppression, we can employ a feature extractor pre-trained on the entire training set (As shown in **Clean Feature Erasing Noise**). However, since our data-constrained backdoor attacks lack access to the complete training set, an alternative solution is required. Recent studies have shown that pre-trained CLIP [46] generates consistent and robust semantic representations across a wide range of (image, text) pairs, enabling impressive zero-shot classification performance comparable to supervised learning accuracy on challenging datasets like ImageNet (As shown in **CLIP for Zero-shot Classification**). Hence, we can utilize the pre-trained general model CLIP, which replaces<sup>§</sup> the feature extractor trained on the entire training set, allowing us to achieve clean feature suppression (As shown in **CLIP for Clean Feature Erasing**).

**Clean feature erasing noise.** The technique of clean feature suppression aims to eliminate the clean information present in images by introducing optimized noise, denoted as  $\delta$ , which helps modify the input image to resemble the unbiased class. In accordance with the data-constrained backdoor attack pipeline outlined in Sec. 3, we assume that the chosen clean training dataset for generating the poisoning set consists of  $P$  clean examples, denoted as  $\mathcal{P}' \subset X \times Y$  (where  $\mathcal{P}' = \{(x_i, y_i) | i = 1, \dots, P\}$ ). Here,  $x_i \in X$  represents the inputs,  $y_i \in Y = \{1, 2, \dots, C\}$  represents the labels, and  $C$  denotes the total number of classes. We refer to the modified version as  $\mathcal{P}_e = \{(x_{e,i}, y_i) | i = 1, \dots, P\}$ , where  $x_{e,i} = x_i + \delta_i$  represents the erased version of the training example  $x_i \in \mathcal{P}'$ . The term  $\delta_i \in \Delta$  denotes the "invisible" noise applied to achieve the erasing effect. The noise  $\delta_i$  is subject to the constraint  $\|\delta_i\|_p \leq \epsilon$ , where  $\|\cdot\|_p$  represents the  $L_p$  norm, and  $\epsilon$  is set to a small value to ensure the stealthiness of the backdoor attacks. Our objective in erasing the clean features is to ensure that the pre-trained feature extractor does not extract any meaningful information from the given images  $x$ . This is achieved by introducing customized and imperceptible noise, denoted as  $\delta_i$ . To be more specific, for a clean example  $x_i$ , we propose to generate the noise  $\delta_i$  that erases the features by solving the following optimization problem:

$$\delta_i = \arg \min_{\delta_i} L(f'(x_i + \delta_i), y_m) \quad \text{s.t.} \quad \|\delta_i\|_p \leq \epsilon, \quad (2)$$

<sup>§</sup>CLIP [46] is a general pre-trained model that has been released by OpenAI. It is pre-trained on 400 million image-text pairs harvested from the Web and can express a much wider set of visual concepts.

where  $L$  represents the mean squared error (MSE) loss, defined as  $L(a, b) = \|a - b\|^2$ . The function  $f'(\cdot)$  corresponds to the pre-trained feature extractor employed for noise generation. Additionally,  $y_m$  denotes the unbiased label for the classification task, which is defined as  $y_m = [\frac{1}{C}, \frac{1}{C}, \dots, \frac{1}{C}]$ , where  $C$  signifies the total number of classes. While this vanilla method proves effective in erasing clean features, it requires a proxy feature extractor that has been pre-trained on the entire training set. This approach is not suitable for our data-restricted backdoor attacks.

**CLIP for zero-shot classification.** The pre-trained CLIP model [46] possesses the ability to express a broader range of visual concepts and has been utilized as a general feature extractor in various tasks. These tasks include text-driven image manipulation [44], zero-shot classification [6], and domain generalization [42]. In this section, we introduce the pipeline of CLIP in zero-shot classification, which can serve as inspiration for incorporating it into our clean feature erasing approach. CLIP achieves zero-shot classification by aligning text and image features. Firstly, CLIP employs its text encoder, denoted as  $\hat{\mathcal{E}}_t(\cdot)$ , to embed the input prompts ("a photo of a  $c_i$ ") into text features  $T_i \in \mathbb{R}^d$ , where  $i = \{1, 2, \dots, C\}$  represents the classes. Subsequently, the image feature  $I_j \in \mathbb{R}^d$  of image  $x_j$  is embedded using the image encoder, denoted as  $\hat{\mathcal{E}}_i(\cdot)$ . During the inference phase, the classification prediction  $y_j$  is computed using the cosine similarity between  $T_i$  and  $I_j$ . This can be expressed as:

$$y_j = \arg \max_i (\langle I_j, T_i \rangle), \quad i \in \{1, 2, \dots, C\}, \quad (3)$$

where  $C$  represents the number of classes, and  $\langle \cdot, \cdot \rangle$  represents the cosine similarity between two vectors.

**CLIP for Clean Feature Erasing (CLIP-CFE).** Taking inspiration from CLIP's approach to zero-shot classification, we leverage a general CLIP model to optimize the feature erasing noise. This allows us to relax the need for a proxy feature extractor pre-trained on the entire training set. We consider  $C$  prompts, "a photo of a  $c_i$ ," corresponding to different classes  $c_i$  in the dataset, where  $i = 1, \dots, C$ . The CLIP-based feature erasing noise, denoted as  $\delta_i$ , is proposed for the input  $x_i$  by solving the following optimization problem:

$$\delta_i = \arg \min_{\delta_i} L(f_{CLIP}(x_i + \delta_i, \mathbb{P}), y_m) \quad \text{s.t.} \quad \|\delta_i\|_p \leq \epsilon, \quad (4)$$

where  $L$  represents the mean squared error (MSE) loss,  $y_m$  denotes the unbiased label for the classification task defined as  $y_m = [\frac{1}{C}, \frac{1}{C}, \dots, \frac{1}{C}]$ ,  $\mathbb{P}$  represents the set of prompts corresponding to different classes in the dataset, and  $f_{CLIP}$  denotes the CLIP-based model used to obtain the label of the input image. Specifically,

$$\mathbb{P} = \{p_1, p_2, \dots, p_C\} = \{"a photo of a  $c_i$ " |  $i = 1, 2, \dots, C\}, \quad (5)$$$



$$f_{CLIP}(x_i + \delta_i, \mathbb{P}) = \left[ \frac{\langle \hat{\mathcal{E}}_i(x_i + \delta_i), \hat{\mathcal{E}}_t(p_1) \rangle}{\sum_{i=1}^C \langle \hat{\mathcal{E}}_i(x_i + \delta_i), \hat{\mathcal{E}}_t(p_i) \rangle}, \dots, \frac{\langle \hat{\mathcal{E}}_i(x_i + \delta_i), \hat{\mathcal{E}}_t(p_C) \rangle}{\sum_{i=1}^C \langle \hat{\mathcal{E}}_i(x_i + \delta_i), \hat{\mathcal{E}}_t(p_i) \rangle} \right]. \quad (6)$$

To solve the constrained minimization problem illustrated in Eq. 4, we utilize the first-order optimization method known as Projected Gradient Descent (PGD) [37]. The PGD method enables us to find a solution by iteratively updating the noise as follows:

$$\delta_i^{t+1} = \prod_{\varepsilon} (\delta_i^t - \alpha \cdot \text{sign}(\nabla_{\delta} L(f_{CLIP}(x_i + \delta_i^t, \mathbb{P}), y_m))), \quad (7)$$

where  $t$  represents the current perturbation step, with a total of  $T = 50$  steps.  $\nabla_{\delta} L(f_{CLIP}(x_i + \delta_i^t, \mathbb{P}), y_m)$  denotes the gradient of the loss with respect to the input. The projection function  $\prod$  is applied to restrict the noise  $\delta$  within the  $\varepsilon$ -ball (with  $\varepsilon = 8/255$  in our paper) around the original example  $x$ , ensuring it does not exceed this boundary. The step size  $\alpha$  determines the magnitude of the noise update at each iteration. The resulting erasing examples are then obtained as follows:

$$\mathcal{P}_e = \{(x_{e,i}, y_i) | i = 1, \dots, P\}, \quad \text{where } x_{e,i} = x_i + \delta_i^T. \quad (8)$$

### 4.3 Poisoning Feature Augmentation

In addition to eradicating clean features in images to tackle the entanglement between benign and poisoning features, enhancing the expression of poisoning features is another effective approach. In this section, we present two parallel triggers aimed at augmenting the poisoning features.

#### 4.3.1 CLIP-based Universal Adversarial Perturbations

In this section, we also employ the widely-used pre-trained CLIP model [46] to generate universal adversarial perturbations as the backdoor trigger. Xia *et al.* [61] argue that deep models inherently possess flaws, and it is easier to exploit and enhance an existing flaw to serve as a backdoor rather than implanting a new one from scratch (BadNets [16] and Blended [5]). Universal Adversarial Perturbations (UAP) [61, 70] utilize these inherent flaws in models as triggers, providing a straightforward method for augmenting the poisoning feature. However, this approach typically requires a feature extractor that has been pre-trained on the entire training set, which is not practical in data-constrained backdoor attacks. To address this limitation, we propose a CLIP-based<sup>§</sup> Universal Adversarial Perturbations (CLIP-UAP) method. Specifically, given an accessible clean training set  $\mathcal{D}' = \{(x_i, y_i) | i = 1, \dots, N'\}$  and an attack-target label  $k$ , the defined trigger can be formulated as follows:

$$\delta_{\text{uap}} = \arg \min_{\|\delta_{\text{uap}}\|_p \leq \varepsilon} \sum_{(x,y) \in \mathcal{D}'} L(f_{CLIP}(x + \delta_{\text{uap}}, \mathbb{P}), k), \quad (9)$$

where  $\mathbb{P}$  and  $f_{CLIP}$  are defined as shown in Eq. 5 and Eq. 6, respectively. Similar to Eq. 7, we utilize the first-order optimization method known as Projected Gradient Descent (PGD) [37] to solve the constrained minimization problem. The optimization process can be expressed as follows:

$$\delta_{\text{uap}}^{t+1} = \prod_{\varepsilon} (\delta_{\text{uap}}^t - \alpha \cdot \text{sign}(\nabla_{\delta_{\text{uap}}} L(f_{CLIP}(x + \delta_{\text{uap}}^t, \mathbb{P}), k))), \quad (10)$$

where  $t$ ,  $\nabla_{\delta_{\text{uap}}} L(f_{CLIP}(x + \delta_{\text{uap}}^t, \mathbb{P}), k)$ , and  $\prod$  hold the same meaning as in Eq. 7. Unlike the sample-wise clean feature erasing noise, the CLIP-UAP serves as a universal trigger for the entire training set. Therefore, it follows the optimization formulation presented in Eq. 10 to generate  $\delta_{\text{uap}}^{t+1}$  at each step  $t$ . The optimization process is performed on all samples in the accessible clean training set  $\mathcal{D}'$ . Consequently, the CLIP-UAP for the set  $\mathcal{D}'$  can be represented as  $\delta_{\text{uap}} = \delta_{\text{uap}}^T$ , and the poison generator is formulated as  $\mathcal{T}(x, \delta_{\text{uap}}) = x + \delta_{\text{uap}}$ .

#### 4.3.2 CLIP-based Contrastive Feature Augmentation

While the CLIP-UAP method has shown impressive results in terms of poisoning efficiency, it requires customization for different attack-target labels. In this section, we propose a more versatile trigger design that is independent of the attack-target label, enhancing the poisoning feature. Drawing inspiration from the entanglement between benign and poisoning features discussed in Sec. 3.5, we utilize contrastive optimization to augment the poisoning feature. Our expectation is that the poisoning feature extracted from the designed trigger will be more expressive compared to the clean feature extracted from the clean samples. Specifically, given a trigger  $\delta_{\text{con}}^{t+1}$  to be optimized, two random views (query:  $x + \delta_{\text{con}}$  and key:  $x_1 + \delta_{\text{con}}$ ) are created by different clean samples ( $x$  and  $x_1$ ). Positive pair is defined as such query-key pair, between different poisoning samples. Negative pairs are defined as pairs between poisoning example and its corresponding clean example, *i.e.* between  $x + \delta_{\text{con}}$  and  $x$ . All views are passed through the pre-trained image encoder  $\hat{\mathcal{E}}_i(\cdot)$  of the CLIP to acquire the representation  $v$ :

$$v_q = \hat{\mathcal{E}}_i(x + \delta_{\text{con}}), \quad v_+ = \hat{\mathcal{E}}_i(x_1 + \delta_{\text{con}}), \quad v_- = \hat{\mathcal{E}}_i(x). \quad (11)$$

CLIP-Contrastive feature augmentation (CLIP-CFA) focuses on optimizing the general trigger by maximizing the similarity between positive pairs while ensuring dissimilarity between negative pairs. To achieve this, we design a loss function as follows:

$$L_{\text{con}}(x, x_1, \delta_{\text{con}}) = -\frac{\langle v_q, v_+ \rangle}{\langle v_q, v_- \rangle}, \quad (12)$$

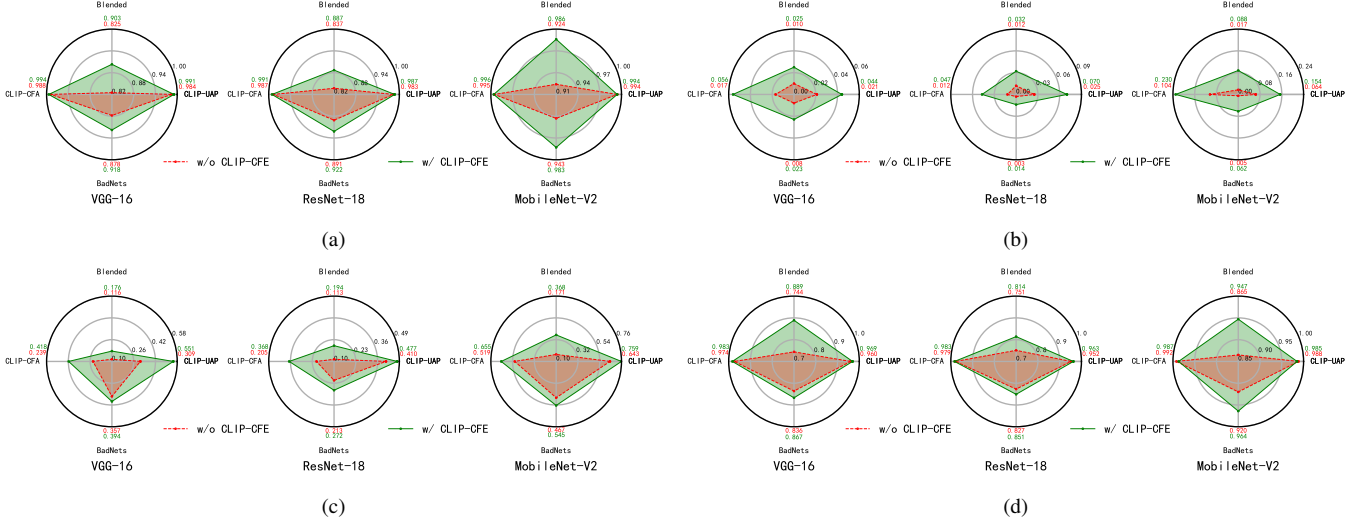


Figure 7: Attack success rate (ASR) of the (a): number-constrained backdoor attacks, (b): clean-label single-class attack (the access category  $Y'$  is set to  $\{0\}$ ), (c): dirty-label single-class attack (the access category  $Y'$  is set to  $\{1\}$ ), and (d): domain-constrained backdoor attacks (domain rate is set to 0) on the CIFAR-100 dataset. The red points represents w/o CLIP-based Clean Feature Erasing (CLIP-CFE), while the green points represents w/ CLIP-CFE. All experiments are repeated 5 times, and the results are computed with the mean of five different runs.

where  $\langle \cdot, \cdot \rangle$  represents the cosine similarity between two vectors and the optimization of  $\delta_{\text{con}}$  is designed as:

$$\delta_{\text{con}} = \arg \min_{\|\delta_{\text{con}}\|_p \leq \epsilon, (x,y) \in \mathcal{D}'} L_{\text{con}}(x, x_1, \delta_{\text{con}}). \quad (13)$$

Similar to Eq. 10, we also adopt the first-order optimization method PGD [37] to solve the constrained minimization problem as follows:

$$\delta_{\text{con}}^{t+1} = \prod_{\epsilon} (\delta_{\text{con}}^t - \alpha \cdot \text{sign}(\nabla_{\delta_{\text{con}}} L_{\text{con}}(x, x_1, \delta_{\text{con}}))). \quad (14)$$

Therefore, the optimization should also be accumulated on all samples in the accessible clean training set  $\mathcal{D}'$ . Finally, the CLIP-CFA of set  $\mathcal{D}'$  can be formulated as  $\delta_{\text{con}} = \delta_{\text{con}}^T$ , and the poison generator is formulated as  $\mathcal{T}(x, \delta_{\text{con}}) = x + \delta_{\text{con}}$ .

#### 4.4 Attack Summary

In Sec. 4.3, we present two independent trigger design methods: CLIP-based Universal Adversarial Perturbations (CLIP-UAP) and CLIP-based Contrastive Feature Augmentation (CLIP-CFA). These triggers are aimed at enhancing the expression of poisoning features and can replace previous trigger design approaches, leading to improved performance in data-constrained backdoor attacks. Additionally, in Sec. 4.2, we introduce a CLIP-based Clean Feature Erasing (CLIP-CFE) method. This approach minimizes the influence of clean features during the poisoning process and can be integrated into any of the aforementioned trigger design methods. By

combining trigger design and clean feature erasing, our final approach achieves state-of-the-art performance in all three types of data-constrained backdoor attacks.

## 5 Experiments

We provide an overview of the experimental settings in this paper, covering various aspects such as datasets, model architecture, evaluation metrics, baselines, and implementations (Appendix 7.1). Subsequently, we perform comprehensive experiments to assess the effectiveness of our proposed methods through answering the following research questions:

**RQ1: Are proposed technologies effective on three backdoor attacks?** (Sec. 5.1)

**RQ2: Are proposed technologies harmless for Benign Accuracy?** (Sec. 5.2)

**RQ3: Are proposed technologies stealthy for victims?** (Sec. 5.3)

**RQ4: Are proposed technologies effective for different poisoning settings?** (Sec. 5.4)

In this section, we present the results specifically for CIFAR-100 datasets. Experimental outcomes for CIFAR-10 and ImageNet-50 are provided in Appendix 7.2 and Appendix 7.3 respectively. Additionally, for further discussions, please refer to Appendix 7.5.

Table 1: The Benign Accuracy (BA) on the CIFAR-100 dataset. All results are computed the mean by 5 different run.

Trigger	Clean Feature Suppression	Backdoor Attacks												Average
		Number Constrained			Class Constrained ( $Y' = \{0\}$ )			Class Constrained ( $Y' = \{1\}$ )			Domain Constrained			
		V-16	R-18	M-2	V-16	R-18	M-2	V-16	R-18	M-2	V-16	R-18	M-2	
BadNets	w/o CLIP-CFE	0.698	0.728	0.722	0.698	0.730	0.728	0.700	0.728	0.729	0.699	0.727	0.728	0.718
	w/ CLIP-CFE	0.700	0.730	0.728	0.701	0.731	0.723	0.698	0.730	0.726	0.701	0.730	0.724	0.719
Blended	w/o CLIP-CFE	0.700	0.727	0.722	0.700	0.726	0.725	0.701	0.729	0.723	0.698	0.729	0.725	0.717
	w/ CLIP-CFE	0.700	0.730	0.727	0.701	0.729	0.727	0.699	0.730	0.724	0.700	0.731	0.727	0.719
CLIP-UAP	w/o CLIP-CFE	0.702	0.730	0.727	0.702	0.729	0.727	0.701	0.730	0.725	0.702	0.731	0.729	0.720
	w/ CLIP-CFE	0.700	0.731	0.725	0.702	0.732	0.726	0.699	0.732	0.724	0.700	0.730	0.725	0.719
CLIP-CFA	w/o CLIP-CFE	0.703	0.731	0.727	0.701	0.730	0.725	0.701	0.730	0.727	0.700	0.731	0.727	0.719
	w/ CLIP-CFE	0.702	0.729	0.729	0.701	0.730	0.727	0.702	0.731	0.725	0.702	0.730	0.727	0.720

### 5.1 RQ1: Are proposed technologies effective on three backdoor attacks?

To assess the effectiveness of our proposed technologies, we conduct attacks on various target models and datasets, evaluating the Attack Success Rate (ASR) for each target model. In order to establish a basis for comparison, we introduce two baseline attack methods: BadNets [16] and Blended [5], as discussed in Sec. 2.1.2. Fig. 7 illustrates the performance of the following types of backdoor attacks on the CIFAR-100 dataset: (a) number-constrained, (b) clean-label single-class (class-constrained), (c) dirty-label single-class (class-constrained), and (d) out-of-the-domain (domain-constrained)<sup>¶</sup>.

**CLIP-based poisoning feature augmentation is more effective than previous attack methods.** Our proposed methods, CLIP-UAP and CLIP-CFA, outperform the baseline techniques (BadNets [16] and Blended [5]<sup>¶</sup>) in terms of consistency across different attacks and target models. Specifically, we achieved an ASR of 0.878, 0.825, 0.984, and 0.988 for BadNets, Blended, CLIP-UAP, and CLIP-CFA, respectively, in the number-constrained backdoor attack on the VGG-16 dataset. These results provide evidence that our proposed poisoning feature augmentation generates more effective triggers compared to other methods.

**CLIP-based Clean Feature Suppression is useful for different attack methods.** Our proposed method, CLIP-CFE, has shown significant improvements in effectiveness compared to the baseline method without CLIP-CFE. In various cases, CLIP-CFE has enhanced the poisoning efficiency significantly. For instance, in the clean-label single-class back-

door attack on the VGG-16 dataset, we observed remarkable improvements of 187%, 150%, 110%, and 229% for BadNets, Blended, CLIP-UAP, and CLIP-CFA, respectively. However, it is worth noting that in the results of the domain-constrained backdoor attacks on MobileNet-V2 (as depicted in the right part of Fig. 7 (d)), CLIP-CFA and CLIP-UAP only slightly outperform the corresponding methods with CFE.

**More discussion.** While our technologies have shown significant improvements in poisoning efficiency compared to baseline methods, there are still important discussions that need to be addressed. We aim to provide answers to the following questions in a systematic manner in Appendix 7.5: i) Why do we observe performance degradation in the clean-label single-class attack? ii) Why are domain-constrained backdoor attacks generally easier compared to class-constrained backdoor attacks?

### 5.2 RQ2: Are proposed technologies harmless for Benign Accuracy?

As shown in Table 1, our proposed methods, CLIP-UAP and CLIP-CFA, exhibit similar or even better average Benign Accuracy (BA) compared to the baseline methods, BadNets [16] and Blended [5]. Additionally, it is worth noting that our proposed method, CLIP-CFE, does not negatively impact BA. This finding confirms that our technologies are harmless to the benign accuracy compared to baseline methods, even under various settings and different backdoor attacks.

### 5.3 RQ3: Are proposed technologies stealthy for victims?

Fig. 8 showcases examples of poisoning images generated by different attacks on the ImageNet-50<sup>\*\*</sup> dataset. While our CLIP-UAP and CLIP-CFA may not achieve the highest stealthiness in terms of SSIM (as indicated in Table 2), the

<sup>¶</sup>Both the clean-label single-class and dirty-label single-class backdoor attacks represent extreme scenarios of the class-constrained backdoor attack. In the clean-label single-class attack, the targeted class category is set to  $Y' = k$ , while in the dirty-label single-class attack, it is set to  $Y' = c$  where  $c \neq k$ . Similarly, the out-of-the-domain backdoor attack is an extreme scenario of the domain-constrained backdoor attack, with a domain rate of 0. For further details, please refer to Appendix 7.1.

<sup>¶</sup>While there are several more effective techniques for poisoning attacks, they typically necessitate access to the entire training data, rendering them unsuitable for our data-limited backdoor attacks.

<sup>\*\*</sup>As shown in Appendix 7.1, CIFAR-10 and CIFAR-100 have low resolution, which makes unclear visualizations. Therefore, we show the results on the ImageNet-50 dataset in this section.

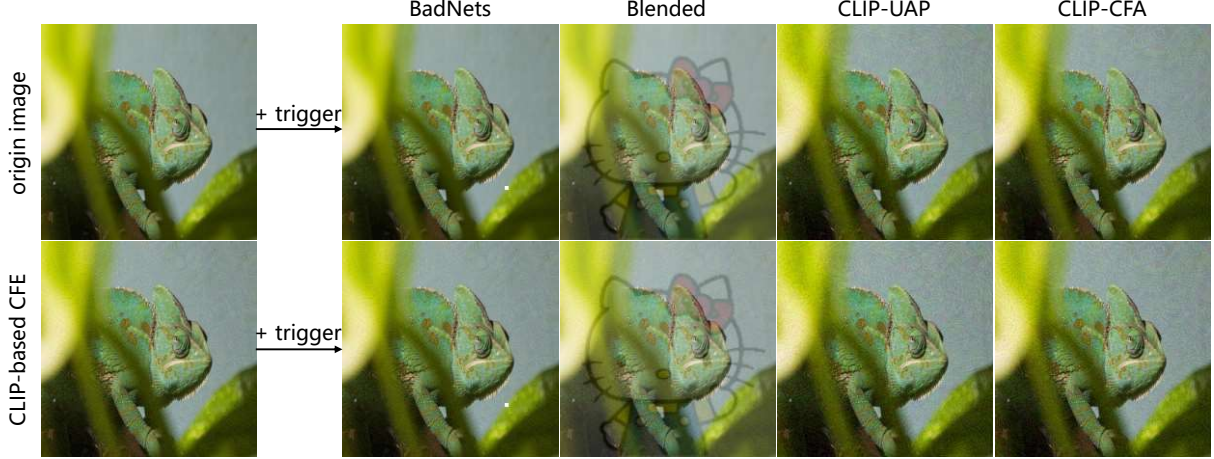


Figure 8: Visualizations of the poisoning samples with different triggers.

Table 2: The Peak Signal-to-noise Ratio (PSNR) and Structural Similarity Index (SSIM) on the ImageNet-50 dataset. All results are computed on the 500 examples.

Metrics	Trigger	Clean Feature Suppression	Backdoor Attacks			
			Number Constrained	Clean-label single-class	Dirty-label single-class	Domain Constrained
PSNR (↑)	BadNets	w/o CLIP-CFE	32.18	31.26	30.91	32.22
		w/ CLIP-CFE	32.19	31.41	31.39	32.17
	Blended	w/o CLIP-CFE	21.68	21.37	20.90	21.60
		w/ CLIP-CFE	21.67	21.31	20.99	21.58
	CLIP-UAP	w/o CLIP-CFE	33.11	33.66	32.84	32.64
		w/ CLIP-CFE	33.10	33.64	32.81	32.59
SSIM (↑)	CLIP-CFA	w/o CLIP-CFE	32.74	32.54	32.70	32.46
		w/ CLIP-CFE	32.72	32.52	32.67	32.41
	BadNets	w/o CLIP-CFE	0.995	0.995	0.995	0.995
		w/ CLIP-CFE	0.995	0.995	0.995	0.995
	Blended	w/o CLIP-CFE	0.794	0.820	0.730	0.787
		w/ CLIP-CFE	0.827	0.834	0.772	0.819
	CLIP-UAP	w/o CLIP-CFE	0.719	0.822	0.641	0.702
		w/ CLIP-CFE	0.843	0.885	0.793	0.822
CLIP-CFA		w/o CLIP-CFE	0.707	0.795	0.637	0.692
		w/ CLIP-CFE	0.830	0.857	0.788	0.810

poisoning images generated by our methods appear more natural to human inspection compared to the baseline attacks. Additionally, incorporating CLIP-CFE has minimal impact on both PSNR and the natural appearance of the images, while achieving higher stealthiness in terms of SSIM.

#### 5.4 RQ4: Are proposed technologies effective for different poisoning settings?

**Experiments on different poison rates for number-constrained backdoor attacks.** We conduct ablation studies to assess the effectiveness of our proposed methods in reducing the number of poisoning samples (poisoning rates) for number-constrained backdoor attacks. The results depicted in Fig. 9 demonstrate the following: i) The attack success rate increases with higher poisoning rates for different attacks. ii) Our proposed CLIP-UAP and CLIP-CFA outperform the

baseline techniques, BadNets [16] and Blended [5]. iii) The incorporation of our proposed CLIP-CFE further enhances the poisoning effectiveness across different triggers.

**Experiments on different poison classes for class-constrained backdoor attacks.** We conduct ablation studies to assess the effectiveness of our proposed methods in increasing the number of poisoning classes for class-constrained backdoor attacks. The results presented in Fig. 10 demonstrate the following: i) The attack success rate increases with higher poisoning classes for different attacks. ii) The attack success rate of clean-label single-class attack is lower than that of dirty-label single-class attacks. iii) Our proposed methods, CLIP-UAP and CLIP-CFA, outperform the baseline techniques, BadNets [16] and Blended [5]. iv) The incorporation of our proposed CLIP-CFE further enhances the poisoning effectiveness across different triggers.

**Experiments on different domain rates for domain-constrained backdoor attacks.** We conduct ablation studies to assess the effectiveness of our methods in increasing the domain rate for domain-constrained backdoor attacks. The results depicted in Fig. 11 demonstrate the following: i) The ASR increases with higher domain rates for different attacks. ii) Our proposed CLIP-UAP and CLIP-CFA outperform the baseline techniques, BadNets [16] and Blended [5]. iii) The incorporation of our proposed CLIP-CFE further enhances the poisoning effectiveness across different triggers.

**Experiments on different large pre-trained models.** We utilize the pre-trained CLIP model as the basis for our technologies. It’s worth noting that the community has proposed various CLIP variants. Therefore, an important practical consideration is whether our proposed technologies remain robust when applied different pre-trained CLIP models. To investigate this, we conduct ablation studies on different CLIP models for number-constrained backdoor attacks, as depicted in Fig. 12. The results demonstrate that our proposed technologies exhibit robustness across different CLIP models, with ViT-B/32 emerging as a competitive choice for all methods.



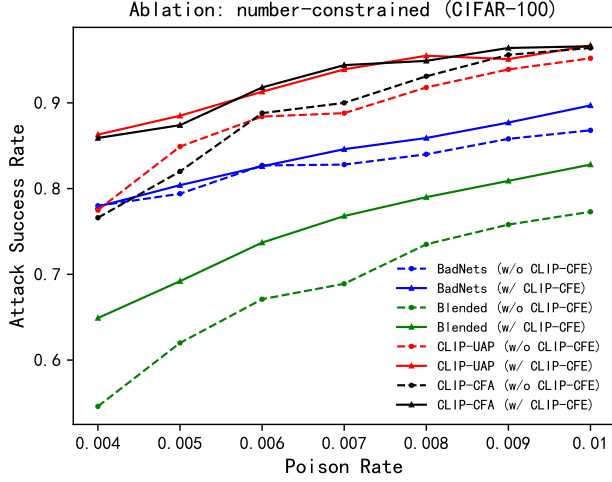


Figure 9: The attack success rate on the CIFAR-100 dataset with different poisoning rates. All results were computed as the mean of five different runs.

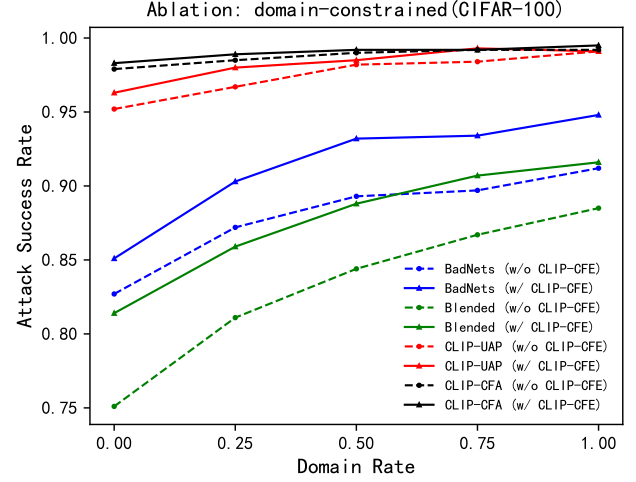


Figure 11: The attack success rate on the CIFAR-100 dataset with different domain rates. All results were computed as the mean of five different runs.

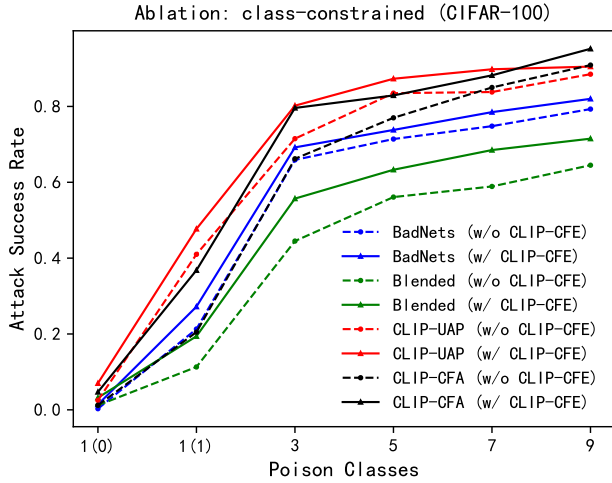


Figure 10: The attack success rate on the CIFAR-100 dataset with different accessible class of poisoning samples, where 1 (0) and 1 (1) in the abscissa represent the clean-label and dirty-label single-class attacks, respectively. All results were computed as the mean of five different runs.

## 6 Limitations and Future Works

In this paper, we address the challenges of data-constrained backdoor attacks, which occur in more realistic scenarios where victims collect data from multiple sources and attackers cannot access the full training data. To overcome the performance degradation observed in previous methods under data-constrained backdoor attacks, we propose three technologies from two streams that leverage the pre-trained CLIP model to enhance the efficiency of poisoning. Our goal is to inspire the research community to explore these realistic backdoor attack scenarios and raise awareness about the threats posed by such attacks. In the following section, we discuss

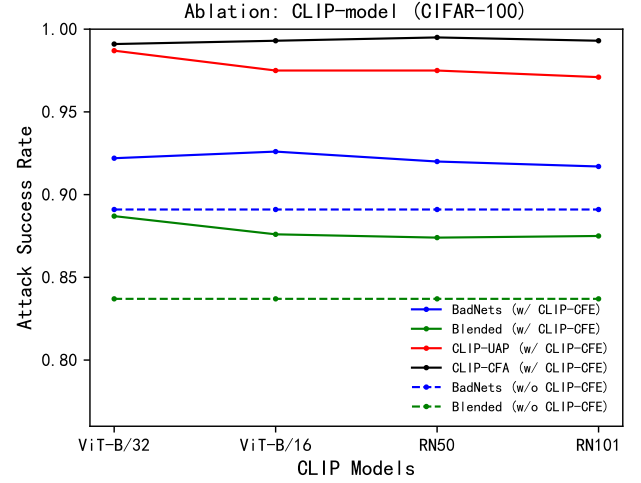


Figure 12: The attack success rate on the CIFAR-100 dataset across different pre-trained CLIP models for number-constrained backdoor attacks. All results are averaged over five separate runs.

the limitations of our approach and outline potential future directions for backdoor learning research.

### Performance degradation in clean-label backdoor attacks.

Clean-label backdoor attacks present a significant challenge [69]. As shown in Fig. 7, previous methods exhibit a poor ASR, and our technologies show limited improvement in clean-label backdoor attacks when the poisoning rate is low. In future research, we will investigate the underlying reasons for this situation and explore more efficient attack methods specifically designed for clean-label backdoor attacks.

**Application limitations.** Our technologies depend on the CLIP model that is pre-trained on natural images, which may limit their applicability to certain domains such as medical images or remote sensing. In such cases, a possible solution

is to replace CLIP with a domain-specific pre-trained model, such as MedCLIP [36] for medical images or Satellite [1] for remote sensing, to adapt our methods to the target domain.

**Transfer to other domains.** The attack scenario we have defined is not limited to a specific domain and can be applied to other important applications, including backdoor attacks for malware detection, deepfake detection, and federated learning. In our future work, we plan to explore the design of realistic attack scenarios and efficient backdoor attacks specifically tailored for these applications.

## References

- [1] Arto, Dev Vidhani, Goutham, Mayank Bhaskar, Ritobrata Ghosh, and Sujit Pal. Fine tuning clip with remote sensing (satellite) images and captions, 2021. <https://huggingface.co/blog/fine-tune-clip-rsacd>.
- [2] Eugene Bagdasaryan and Vitaly Shmatikov. Blind backdoors in deep learning models. In *30th USENIX Security Symposium (USENIX Security 21)*, pages 1505–1521, 2021.
- [3] Tom Brown, Benjamin Mann, Nick Ryder, Melanie Subbiah, Jared D Kaplan, Prafulla Dhariwal, Arvind Neelakantan, Pranav Shyam, Girish Sastry, Amanda Askell, et al. Language models are few-shot learners. *Advances in neural information processing systems*, 33:1877–1901, 2020.
- [4] Huili Chen, Cheng Fu, Jishen Zhao, and Farinaz Koushanfar. Proflip: Targeted trojan attack with progressive bit flips. In *Proceedings of the IEEE/CVF International Conference on Computer Vision*, pages 7718–7727, 2021.
- [5] Xinyun Chen, Chang Liu, Bo Li, Kimberly Lu, and Dawn Song. Targeted backdoor attacks on deep learning systems using data poisoning. *arXiv preprint arXiv:1712.05526*, 2017.
- [6] Ruizhe Cheng, Bichen Wu, Peizhao Zhang, Peter Vajda, and Joseph E Gonzalez. Data-efficient language-supervised zero-shot learning with self-distillation. In *Proceedings of the IEEE/CVF Conference on Computer Vision and Pattern Recognition*, pages 3119–3124, 2021.
- [7] Siyuan Cheng, Yingqi Liu, Shiqing Ma, and Xiangyu Zhang. Deep feature space trojan attack of neural networks by controlled detoxification. In *Proceedings of the AAAI Conference on Artificial Intelligence*, volume 35, pages 1148–1156, 2021.
- [8] Jia Deng, Wei Dong, Richard Socher, Li-Jia Li, Kai Li, and Li Fei-Fei. Imagenet: A large-scale hierarchical image database. In *2009 IEEE conference on computer vision and pattern recognition*, pages 248–255. Ieee, 2009.
- [9] Khoa Doan, Yingjie Lao, and Ping Li. Backdoor attack with imperceptible input and latent modification. *Advances in Neural Information Processing Systems*, 34:18944–18957, 2021.
- [10] Jacob Dumford and Walter Scheirer. Backdooring convolutional neural networks via targeted weight perturbations. In *2020 IEEE International Joint Conference on Biometrics (IJCB)*, pages 1–9. IEEE, 2020.
- [11] Muhammad Farooq and Abdul Hafeez. Covid-resnet: A deep learning framework for screening of covid19 from radiographs. *arXiv preprint arXiv:2003.14395*, 2020.
- [12] Yu Feng, Benteng Ma, Jing Zhang, Shanshan Zhao, Yong Xia, and Dacheng Tao. Fiba: Frequency-injection based backdoor attack in medical image analysis. In *Proceedings of the IEEE/CVF Conference on Computer Vision and Pattern Recognition*, pages 20876–20885, 2022.
- [13] Yansong Gao, Bao Gia Doan, Zhi Zhang, Siqi Ma, Jiliang Zhang, Anmin Fu, Surya Nepal, and Hyoungshick Kim. Backdoor attacks and countermeasures on deep learning: A comprehensive review. *arXiv preprint arXiv:2007.10760*, 2020.
- [14] Yunjie Ge, Qian Wang, Baolin Zheng, Xinlu Zhuang, Qi Li, Chao Shen, and Cong Wang. Anti-distillation backdoor attacks: Backdoors can really survive in knowledge distillation. In *Proceedings of the 29th ACM International Conference on Multimedia*, pages 826–834, 2021.
- [15] Micah Goldblum, Dimitris Tsipras, Chulin Xie, Xinyun Chen, Avi Schwarzschild, Dawn Song, Aleksander Madry, Bo Li, and Tom Goldstein. Dataset security for machine learning: Data poisoning, backdoor attacks, and defenses. *IEEE Transactions on Pattern Analysis and Machine Intelligence*, 2022.
- [16] Tianyu Gu, Kang Liu, Brendan Dolan-Gavitt, and Siddharth Garg. Badnets: Evaluating backdooring attacks on deep neural networks. *IEEE Access*, 7:47230–47244, 2019.
- [17] Kaiming He, Xiangyu Zhang, Shaoqing Ren, and Jian Sun. Deep residual learning for image recognition. In *Proceedings of the IEEE conference on computer vision and pattern recognition*, pages 770–778, 2016.
- [18] Sanghyun Hong, Pietro Frigo, Yiğitcan Kaya, Cristiano Giuffrida, and Tudor Dumitras. Terminal brain damage: Exposing the graceless degradation in deep neural networks under hardware fault attacks. In *28th USENIX Security Symposium (USENIX Security 19)*, pages 497–514, 2019.
- [19] Quan Huynh-Thu and Mohammed Ghanbari. Scope of validity of psnr in image/video quality assessment. *Electronics letters*, 44(13):800–801, 2008.
- [20] Tero Karras, Samuli Laine, and Timo Aila. A style-based generator architecture for generative adversarial networks. In *Proceedings of the IEEE/CVF conference on computer vision and pattern recognition*, pages 4401–4410, 2019.
- [21] Daniel Keysers, Thomas Deselaers, Christian Gollan, and Hermann Ney. Deformation models for image recognition. *IEEE Transactions on Pattern Analysis and Machine Intelligence*, 29(8):1422–1435, 2007.
- [22] Alex Krizhevsky, Geoffrey Hinton, et al. Learning multiple layers of features from tiny images. 2009.
- [23] Keita Kurita, Paul Michel, and Graham Neubig. Weight poisoning attacks on pre-trained models. *arXiv preprint arXiv:2004.06660*, 2020.
- [24] Chaoran Li, Xiao Chen, Derui Wang, Sheng Wen, Muhammad Ejaz Ahmed, Seyit Camtepe, and Yang Xiang. Backdoor attack on machine learning based android malware detectors. *IEEE Transactions on Dependable and Secure Computing*, 19(5):3357–3370, 2021.
- [25] Shaofeng Li, Hui Liu, Tian Dong, Benjamin Zi Hao Zhao, Minhui Xue, Haojin Zhu, and Jialiang Lu. Hidden backdoors in human-centric language models. In *Proceedings of the 2021*

*ACM SIGSAC Conference on Computer and Communications Security*, pages 3123–3140, 2021.

- [26] Shaofeng Li, Minhui Xue, Benjamin Zi Hao Zhao, Haojin Zhu, and Xinpeng Zhang. Invisible backdoor attacks on deep neural networks via steganography and regularization. *IEEE Transactions on Dependable and Secure Computing*, 18(5):2088–2105, 2020.
- [27] Yiming Li, Yong Jiang, Zhifeng Li, and Shu-Tao Xia. Backdoor learning: A survey. *IEEE Transactions on Neural Networks and Learning Systems*, 2022.
- [28] Yuanchun Li, Jiayi Hua, Haoyu Wang, Chunyang Chen, and Yunxin Liu. Deeppayload: Black-box backdoor attack on deep learning models through neural payload injection. In *2021 IEEE/ACM 43rd International Conference on Software Engineering (ICSE)*, pages 263–274. IEEE, 2021.
- [29] Yuezun Li, Yiming Li, Baoyuan Wu, Longkang Li, Ran He, and Siwei Lyu. Invisible backdoor attack with sample-specific triggers. In *Proceedings of the IEEE/CVF International Conference on Computer Vision*, pages 16463–16472, 2021.
- [30] Ziqiang Li, Muhammad Usman, Rentuo Tao, Pengfei Xia, Chaoyue Wang, Huanhuan Chen, and Bin Li. A systematic survey of regularization and normalization in gans. *ACM Comput. Surv.*, 55(11), 2023.
- [31] Ziqiang Li, Pengfei Xia, Xue Rui, and Bin Li. Exploring the effect of high-frequency components in gans training. *ACM Transactions on Multimedia Computing, Communications and Applications*, 19(5):1–22, 2023.
- [32] Cong Liao, Haoti Zhong, Anna Squicciarini, Sencun Zhu, and David Miller. Backdoor embedding in convolutional neural network models via invisible perturbation. *arXiv preprint arXiv:1808.10307*, 2018.
- [33] Pengfei Liu, Weizhe Yuan, Jinlan Fu, Zhengbao Jiang, Hiroaki Hayashi, and Graham Neubig. Pre-train, prompt, and predict: A systematic survey of prompting methods in natural language processing. *ACM Computing Surveys*, 55(9):1–35, 2023.
- [34] Yingqi Liu, Shiqing Ma, Yousra Aafer, Wen-Chuan Lee, Juan Zhai, Weihang Wang, and Xiangyu Zhang. Trojaning attack on neural networks. 2017.
- [35] Yunfei Liu, Xingjun Ma, James Bailey, and Feng Lu. Reflection backdoor: A natural backdoor attack on deep neural networks. In *European Conference on Computer Vision*, pages 182–199. Springer, 2020.
- [36] Kaushalya Madhawa and Raul Carlomagno. Medclip: A pre-trained clip model for medical image search, 2022. <https://github.com/Kaushalya/medclip>.
- [37] Aleksander Madry, Aleksandar Makelov, Ludwig Schmidt, Dimitris Tsipras, and Adrian Vladu. Towards deep learning models resistant to adversarial attacks. *arXiv preprint arXiv:1706.06083*, 2017.
- [38] Seyed-Mohsen Moosavi-Dezfooli, Alhussein Fawzi, Omar Fawzi, and Pascal Frossard. Universal adversarial perturbations. In *Proceedings of the IEEE conference on computer vision and pattern recognition*, pages 1765–1773, 2017.
- [39] Anh Nguyen and Anh Tran. Wanet-imperceptible warping-based backdoor attack. *arXiv preprint arXiv:2102.10369*, 2021.
- [40] Thien Duc Nguyen, Phillip Rieger, Markus Miettinen, and Ahmad-Reza Sadeghi. Poisoning attacks on federated learning-based iot intrusion detection system. In *Proc. Workshop Decentralized IoT Syst. Secur.(DISS)*, pages 1–7, 2020.
- [41] Tuan Anh Nguyen and Anh Tran. Input-aware dynamic backdoor attack. *Advances in Neural Information Processing Systems*, 33:3454–3464, 2020.
- [42] Hongjing Niu, Hanting Li, Feng Zhao, and Bin Li. Domain-unified prompt representations for source-free domain generalization. *arXiv preprint arXiv:2209.14926*, 2022.
- [43] Xudong Pan, Mi Zhang, Beina Sheng, Jiaming Zhu, and Min Yang. Hidden trigger backdoor attack on {NLP} models via linguistic style manipulation. In *31st USENIX Security Symposium (USENIX Security 22)*, pages 3611–3628, 2022.
- [44] Or Patashnik, Zongze Wu, Eli Shechtman, Daniel Cohen-Or, and Dani Lischinski. Styleclip: Text-driven manipulation of stylegan imagery. In *Proceedings of the IEEE/CVF International Conference on Computer Vision*, pages 2085–2094, 2021.
- [45] Junyang Qiu, Jun Zhang, Wei Luo, Lei Pan, Surya Nepal, and Yang Xiang. A survey of android malware detection with deep neural models. *ACM Computing Surveys (CSUR)*, 53(6):1–36, 2020.
- [46] Alec Radford, Jong Wook Kim, Chris Hallacy, Aditya Ramesh, Gabriel Goh, Sandhini Agarwal, Girish Sastry, Amanda Askell, Pamela Mishkin, Jack Clark, et al. Learning transferable visual models from natural language supervision. In *International conference on machine learning*, pages 8748–8763. PMLR, 2021.
- [47] Adnan Siraj Rakin, Zhezhi He, and Deliang Fan. Tbt: Targeted neural network attack with bit trojan. In *Proceedings of the IEEE/CVF Conference on Computer Vision and Pattern Recognition*, pages 13198–13207, 2020.
- [48] Goutham Ramakrishnan and Aws Albarghouthi. Backdoors in neural models of source code. *arXiv preprint arXiv:2006.06841*, 2020.
- [49] Robin Rombach, Andreas Blattmann, Dominik Lorenz, Patrick Esser, and Björn Ommer. High-resolution image synthesis with latent diffusion models. In *Proceedings of the IEEE/CVF Conference on Computer Vision and Pattern Recognition*, pages 10684–10695, 2022.
- [50] Aniruddha Saha, Akshayvarun Subramanya, and Hamed Pirsiavash. Hidden trigger backdoor attacks. In *Proceedings of the AAAI conference on artificial intelligence*, volume 34, pages 11957–11965, 2020.
- [51] Mark Sandler, Andrew Howard, Menglong Zhu, Andrey Zhmoginov, and Liang-Chieh Chen. Mobilenetv2: Inverted residuals and linear bottlenecks. In *Proceedings of the IEEE conference on computer vision and pattern recognition*, pages 4510–4520, 2018.
- [52] Karen Simonyan and Andrew Zisserman. Very deep convolutional networks for large-scale image recognition. *arXiv preprint arXiv:1409.1556*, 2014.
- [53] Hossein Souri, Micah Goldblum, Liam Fowl, Rama Chellappa, and Tom Goldstein. Sleeper agent: Scalable hidden trigger

backdoors for neural networks trained from scratch. *arXiv preprint arXiv:2106.08970*, 2021.

- [54] Alexander Turner, Dimitris Tsipras, and Aleksander Madry. Label-consistent backdoor attacks. *arXiv preprint arXiv:1912.02771*, 2019.
- [55] Cheng Wang, Delei Chen, Lin Hao, Xuebo Liu, Yu Zeng, Jianwei Chen, and Guokai Zhang. Pulmonary image classification based on inception-v3 transfer learning model. *IEEE Access*, 7:146533–146541, 2019.
- [56] Shuo Wang, Surya Nepal, Carsten Rudolph, Marthie Grobler, Shangyu Chen, and Tianle Chen. Backdoor attacks against transfer learning with pre-trained deep learning models. *IEEE Transactions on Services Computing*, 2020.
- [57] Zhou Wang, Alan C Bovik, Hamid R Sheikh, and Eero P Simoncelli. Image quality assessment: from error visibility to structural similarity. *IEEE transactions on image processing*, 13(4):600–612, 2004.
- [58] Long Wen, Xinyu Li, and Liang Gao. A transfer convolutional neural network for fault diagnosis based on resnet-50. *Neural Computing and Applications*, 32:6111–6124, 2020.
- [59] Tong Wu, Tianhao Wang, Vikash Sehwal, Saeed Mahloujifar, and Prateek Mittal. Just rotate it: Deploying backdoor attacks via rotation transformation. *arXiv preprint arXiv:2207.10825*, 2022.
- [60] Pengfei Xia, Ziqiang Li, Wei Zhang, and Bin Li. Data-efficient backdoor attacks. *arXiv preprint arXiv:2204.12281*, 2022.
- [61] Pengfei Xia, Yueqi Zeng, Ziqiang Li, Wei Zhang, and Bin Li. Efficient trojan injection: 90% attack success rate using 0.04% poisoned samples, 2023.
- [62] Xiaoling Xia, Cui Xu, and Bing Nan. Inception-v3 for flower classification. In *2017 2nd international conference on image, vision and computing (ICIVC)*, pages 783–787. IEEE, 2017.
- [63] Runhua Xu, James BD Joshi, and Chao Li. Cryptonn: Training neural networks over encrypted data. In *2019 IEEE 39th International Conference on Distributed Computing Systems (ICDCS)*, pages 1199–1209. IEEE, 2019.
- [64] Limin Yang, Wenbo Guo, Qingying Hao, Arridhana Ciptadi, Ali Ahmadzadeh, Xinyu Xing, and Gang Wang. Cade: Detecting and explaining concept drift samples for security applications. In *USENIX security symposium*, pages 2327–2344, 2021.
- [65] Yi Zeng, Minzhou Pan, Hoang Anh Just, Lingjuan Lyu, Meikang Qiu, and Ruoxi Jia. Narcissus: A practical clean-label backdoor attack with limited information. *arXiv preprint arXiv:2204.05255*, 2022.
- [66] Yi Zeng, Won Park, Z Morley Mao, and Ruoxi Jia. Rethinking the backdoor attacks’ triggers: A frequency perspective. In *Proceedings of the IEEE/CVF International Conference on Computer Vision*, pages 16473–16481, 2021.
- [67] Tongqing Zhai, Yiming Li, Ziqi Zhang, Baoyuan Wu, Yong Jiang, and Shu-Tao Xia. Backdoor attack against speaker verification. In *ICASSP 2021-2021 IEEE International Conference on Acoustics, Speech and Signal Processing (ICASSP)*, pages 2560–2564. IEEE, 2021.

[68] Liping Zhao, Waad Alhoshan, Alessio Ferrari, Keletso J Letsholo, Muideen A Ajagbe, Erol-Valeriu Chioasca, and Riza T Batista-Navarro. Natural language processing for requirements engineering: A systematic mapping study. *ACM Computing Surveys (CSUR)*, 54(3):1–41, 2021.

[69] Shihao Zhao, Xingjun Ma, Xiang Zheng, James Bailey, Jingjing Chen, and Yu-Gang Jiang. Clean-label backdoor attacks on video recognition models. In *Proceedings of the IEEE/CVF Conference on Computer Vision and Pattern Recognition*, pages 14443–14452, 2020.

[70] Haoti Zhong, Cong Liao, Anna Cinzia Squicciarini, Sencun Zhu, and David Miller. Backdoor embedding in convolutional neural network models via invisible perturbation. In *Proceedings of the Tenth ACM Conference on Data and Application Security and Privacy*, pages 97–108, 2020.

## 7 Appendix

### 7.1 Experimental Setup

#### 7.1.1 Datasets

We use the following three popular datasets in image classification: **CIFAR-10** [22]. CIFAR-10 is a tiny object classification dataset containing 50,000 training images and 10,000 testing images. Each image has a size of  $32 \times 32 \times 3$  and belongs to one of 10 classes.

**CIFAR-100** [22]. Similar to CIFAR-10, CIFAR-100 is also a tiny object classification dataset containing 50,000 training images and 10,000 testing images. Each image has a size of  $32 \times 32 \times 3$  and belongs to one of 100 classes.

**ImageNet-50** [8]. ImageNet is the most popular object classification dataset containing 1.3M training images and 50K testing images. Each image has a size of  $224 \times 224 \times 3$  and belongs to one of 1000 classes. For simplicity, we randomly sampled 50 categories to compose a tiny dataset: ImageNet-50. Our ImageNet-50 dataset contains 60K training images and 2.5K testing images.

#### 7.1.2 Model Architecture.

We verify the performance on three popular model architectures of image classification: **VGG-16** [52], **ResNet-18** [17], and **MobileNet-V2** [51]. All of them are widely used in various areas of artificial intelligence, such as flower classification [62], pulmonary image classification [55], fault diagnosis [58], and Covid-19 screening [11].

#### 7.1.3 Baseline and Comparison.

Our method contains two aspects: clean feature suppression and poisoning feature augmentation. Among them, poisoning feature augmentation can be accomplished through designing efficient and data-independent triggers, while clean feature suppression is orthogonal to previous trigger designing and can be integrated into any backdoor triggers. Therefore, we compare our two designed triggers CLIP-based universal adversarial perturbations (CLIP-UAP) and CLIP-based contrastive feature augmentation (CLIP-CFA) with two popular triggers: BadNets [16] and Blended [5]. All of them are independent of the training data therefore can be implemented easily in the introduced data-constrained backdoor attacks. To verify the validity of the clean feature suppression, we integrate the



proposed CLIP-based clean feature erasing (CLIP-CFE) onto currently designed triggers: two our designed triggers and two baseline triggers.

### 7.1.4 Implementations.

In order to demonstrate the effectiveness of our proposed method, we conduct experiments on three datasets (CIFAR-10, CIFAR-100, and ImageNet-50). For the CIFAR-10 and CIFAR-100 datasets, we choose VGG-16, ResNet-18, and MobileNet-V2 as the victim models. All models use the SGD optimizer with a momentum of 0.9, weight decay of  $5e-4$ , and a learning rate of 0.01 (0.1 for MobileNet-V2), which is multiplied by 0.1 at epoch 35 and 55. For the ImageNet-50 dataset, we use VGG-16 and MobileNet-V2 as the victim models. We use the SGD optimizer with a momentum of 0.9, weight decay of  $5e-4$ , and a learning rate of 0.05 (0.01 for VGG-16), which is multiplied by 0.1 at epoch 35 and 55. The complete training epochs is 70.

In the number-constrained scenario, we conducted experiments with poisoning rates of 0.01 ( $P=500$ ), 0.015 ( $P=750$ ), and 0.007 ( $P=453$ ) for the CIFAR10, CIFAR100, and ImageNet-50 three datasets, respectively. In the class-constrained scenario, experiments with poisoning rates of 0.02 ( $P=1000$ ), 0.01 ( $P=500$ ), and 0.02 ( $P=1296$ ) for three datasets. We choose two extreme scenario in the class-constrained backdoor attacks, denoted as clean-label single-class backdoor attack and dirty-label single-class backdoor attack. Specifically, the accessed class category is set to  $Y' = \{k\}$  and  $Y' = \{c\}$ ,  $c \neq k$  for clean-label single-class backdoor attack and dirty-label single-class backdoor attack, respectively. In the domain-constrained scenario, experiments with poisoning rates of 0.02 ( $P=1000$ , 1000, and 1296) for three datasets. The out-of-domain samples of all experiments are selected from other ImageNet-1K datasets that are not ImageNet-50. The attack-target class  $k$  is set to category 0 for all experiments of above three data-constrained backdoor attacks.

### 7.1.5 Evaluation Metrics.

We evaluate the performance of our method in terms of *Harmlessness*: **Benign Accuracy (BA)**, *Effectiveness*: **Attack Success Rate (ASR)**, and *Stealthiness*: **Peak Signal-to-noise Ratio (PSNR)** [19] and **Structural Similarity Index (SSIM)** [57].

**Benign Accuracy (BA).** BA is the clean accuracy of the testing set  $\mathcal{D}_t = \{(x_i, y_i) | i = 1, \dots, M\}$  and is applied to evaluate the *Harmlessness* of the backdoor. When BA of the infected model is similar to the accuracy of the clean model, we believe that the current attack technique is harmless.

**Attack Success Rate (ASR).** ASR is applied to evaluate the *effectiveness* of the backdoor attack, which is the fraction of testing images with specific trigger that are predicted as the target class. Specifically, For  $M'$  images in the testing set that do not belong to the attack-target class ( $k$ ), the ASR is formulated as:

$$\text{ASR} = \frac{\sum_{i=1}^{M'} \mathbb{I}(f(\mathcal{T}(x_i, t); \Theta) = k)}{M'}, \quad (x_i, y_i) \in \mathcal{D}'_t, \quad (15)$$

where  $\mathcal{D}'_t$  is a subset of testing set  $\mathcal{D}_t$  ( $\mathcal{D}'_t \subset \mathcal{D}_t$ ), containing the images whose label is not the attack-target class  $k$ .

**Peak Signal-to-noise Ratio (PSNR)** [19]. PSNR is applied to measure the similarity between clean images and the corresponding

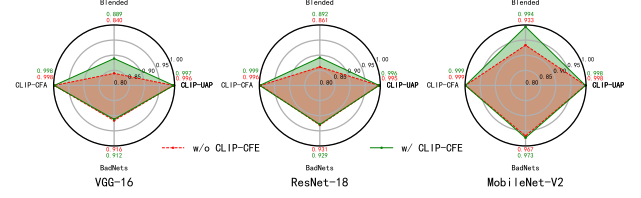


Figure 13: Attack success rate (ASR) of the number-constrained backdoor attacks on the CIFAR-10 dataset. The red points represents w/o CLIP-based Clean Feature Erasing (CFE), while the green points represents w/ CLIP-based Clean Feature Erasing (CFE). The experiment is repeated 5 times, and the results were computed as the mean of five different runs.

poisoning images. Give a image  $x_i \in \mathcal{D}_t$  and the corresponding poisoning image  $x'_i = \mathcal{T}(x_i, t)$ , the PSNR is formulated as:

$$\text{PSNR} = \frac{1}{M} \sum_{i=1}^M \text{PSNR}_i(x_i, x'_i),$$

where  $\text{PSNR}_i(x_i, x'_i) = 10 \log_{10} \left( 255^2 / \text{MSE}(x_i, x'_i) \right)$ , (16)

$$\text{MSE}(f, g) = \frac{1}{HW} \sum_{i=1}^H \sum_{j=1}^W (f_{ij} - g_{ij})^2,$$

$H$  and  $W$  are height and width of the image, respectively. Larger PSNR means larger similarity between clean images and the corresponding poisoning images, therefore larges stealthiness of backdoor attacks.

**Structural Similarity Index (SSIM)** [57]. Similar to PSNR, SSIM is another metrics to represent the stealthiness of backdoor attacks, which is formulated as:

$$\text{SSIM} = \frac{1}{M} \sum_{i=1}^M \text{SSIM}_i(x_i, x'_i),$$

where  $\text{SSIM}_i(x_i, x'_i) = l(x_i, x'_i) \cdot c(x_i, x'_i) \cdot s(x_i, x'_i)$ , (17)

$$\begin{cases} l(f, g) = \frac{2\mu_f\mu_g + C_1}{\mu_f^2 + \mu_g^2 + C_1} \\ c(f, g) = \frac{2\sigma_f\sigma_g + C_2}{\sigma_f^2 + \sigma_g^2 + C_2} \\ s(f, g) = \frac{\sigma_{fg} + C_3}{\sigma_f\sigma_g + C_3} \end{cases},$$

where  $\mu$  and  $\sigma$  are mean and variance of image, respectively. Similarly, Larger SSIM means larger similarity between clean images and the corresponding poisoning images, therefore larges stealthiness of backdoor attacks.

## 7.2 Experiments on the CIFAR-10 Dataset

### 7.2.1 RQ1: Are proposed technologies effective on different backdoor attacks.

In this section, we utilize our proposed technologies to attack different target models on the CIFAR-10 dataset. Our objective is to verify the effectiveness of the attack and calculate the ASR for each target model. The baseline attack methods, BadNets [16] and Blended [5] were introduced in Sec. 2.1.2. The attack performance of the number-constrained, clean-label single-class (class-constrained),

Table 3: The Benign Accuracy (BA) on the CIFAR-10 dataset. All results are computed the mean by 5 different run.

Trigger	Clean Feature Suppression	Backdoor Attacks											
		Number Constrained			Class Constrained ( $Y' = \{0\}$ )			Class Constrained ( $Y' = \{1\}$ )			Domain Constrained		
		V-16	R-18	M-2	V-16	R-18	M-2	V-16	R-18	M-2	V-16	R-18	M-2
BadNets	w/o CLIP-CFE	0.920	0.926	0.928	0.921	0.928	0.928	0.923	0.928	0.928	0.921	0.928	0.929
	w/ CLIP-CFE	0.920	0.927	0.928	0.920	0.927	0.928	0.920	0.926	0.927	0.920	0.927	0.928
Blended	w/o CLIP-CFE	0.921	0.927	0.930	0.921	0.928	0.929	0.919	0.928	0.928	0.920	0.926	0.929
	w/ CLIP-CFE	0.921	0.926	0.929	0.921	0.927	0.929	0.920	0.927	0.929	0.921	0.927	0.929
CLIP-UAP	w/o CLIP-CFE	0.922	0.928	0.927	0.921	0.928	0.928	0.920	0.928	0.928	0.920	0.930	0.928
	w/ CLIP-CFE	0.922	0.928	0.929	0.922	0.928	0.929	0.920	0.927	0.929	0.922	0.928	0.928
CLIP-CFA	w/o CLIP-CFE	0.922	0.928	0.928	0.921	0.927	0.927	0.920	0.928	0.928	0.921	0.929	0.928
	w/ CLIP-CFE	0.922	0.929	0.927	0.920	0.927	0.928	0.921	0.929	0.929	0.921	0.929	0.928

Table 4: The Benign Accuracy (BA) on the ImageNet-50 dataset. All results are computed the mean by 5 different run.

Trigger	Clean Feature Suppression	Backdoor Attacks							
		Number Constrained		Class Constrained ( $Y' = \{0\}$ )		Class Constrained ( $Y' = \{1\}$ )		Domain Constrained	
		V-16	M-2	V-16	M-2	V-16	M-2	V-16	M-2
BadNets	w/o CLIP-CFE	0.784	0.731	0.788	0.731	0.788	0.733	0.783	0.735
	w/ CLIP-CFE	0.787	0.733	0.788	0.735	0.790	0.734	0.788	0.735
Blended	w/o CLIP-CFE	0.789	0.733	0.788	0.736	0.787	0.727	0.788	0.731
	w/ CLIP-CFE	0.790	0.731	0.787	0.734	0.788	0.731	0.786	0.728
CLIP-UAP	w/o CLIP-CFE	0.788	0.729	0.788	0.726	0.786	0.728	0.789	0.733
	w/ CLIP-CFE	0.785	0.732	0.786	0.729	0.786	0.734	0.791	0.730
CLIP-CFA	w/o CLIP-CFE	0.784	0.730	0.789	0.732	0.785	0.729	0.787	0.735
	w/ CLIP-CFE	0.787	0.732	0.786	0.734	0.789	0.735	0.784	0.732

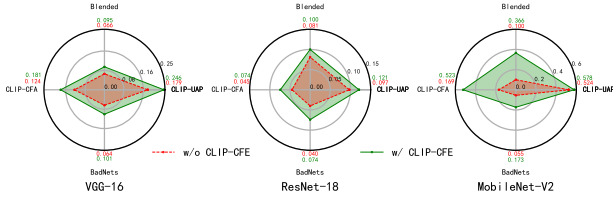


Figure 14: The attack success rate (ASR) of the class-constrained backdoor attacks (the access category  $Y'$  is set to  $\{0\}$ ) on the CIFAR-10 dataset. The red points represents w/o CLIP-based Clean Feature Erasing (CFE), while the green points represents w/ CLIP-based Clean Feature Erasing (CFE). The experiment is repeated 5 times, and the results were computed as the mean of five different runs.

dirty-label single-class (class-constrained), and out-of-the-domain (domain-constrained) backdoor attacks on CIFAR-10 dataset are reflected in Fig. 13, 14, 15, and 16, respectively.

**CLIP-based Poisoning Feature Augmentation Is More Effective Than Previous Attack Methods.** Our proposed CLIP-UAP and CLIP-CFA methods outperform the BadNets [16] and Blended [5] baseline methods in terms of consistency under different attacks and datasets. This confirms that the proposed poisoning feature augmentation generates more efficient triggers than other methods.

**CLIP-based Clean Feature Suppression Is Useful For Different Attack Methods.** Our proposed CLIP-CFE method improves the poisoning effectiveness on most cases compared to the baseline

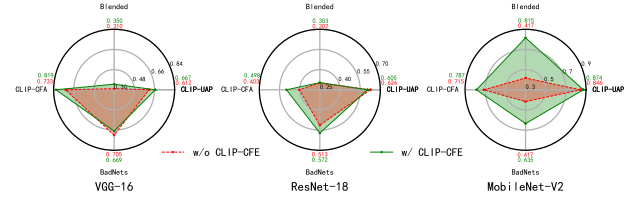


Figure 15: The attack success rate (ASR) of the class-constrained backdoor attacks (the access category  $Y'$  is set to  $\{1\}$ ) on the CIFAR-10 dataset. The red points represents w/o CLIP-based Clean Feature Erasing (CFE), while the green points represents w/ CLIP-based Clean Feature Erasing (CFE). The experiment is repeated 5 times, and the results were computed as the mean of five different runs.

without CLIP-based Clean Feature Erasing. Only on small cases the BadNets and CLIP-UAP slightly outperform the corresponding methods with CFE.

## 7.2.2 RQ2: Are proposed three technologies harmless for Benign Accuracy.

Table 3 illustrates that our proposed CLIP-UAP and CLIP-CFA methods have similar or even better average Benign Accuracy (BA) compared to the baseline methods BadNets [16] and Blended [5]. Additionally, our proposed CLIP-CFE method has no negative effect on BA, confirming that our technologies are harmless for benign

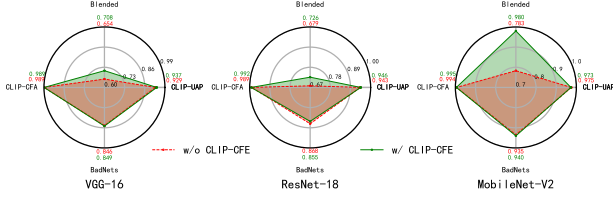


Figure 16: The attack success rate (ASR) of the domain-constrained backdoor attacks (Domain rate is set to 0) on the CIFAR-10 dataset. The red points represents w/o CLIP-based Clean Feature Erasing (CFE), while the green points represents w/ CLIP-based Clean Feature Erasing (CFE). The experiment is repeated 5 times, and the results were computed as the mean of five different runs.

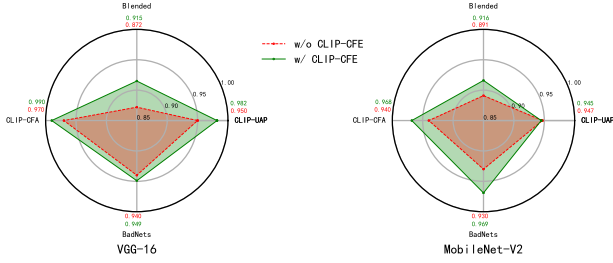


Figure 17: Attack success rate (ASR) of the number-constrained backdoor attacks on the ImageNet-50 dataset. The red points represents w/o CLIP-based Clean Feature Erasing (CFE), while the green points represents w/ CLIP-based Clean Feature Erasing (CFE). The experiment is repeated 5 times, and the results were computed as the mean of five different runs.

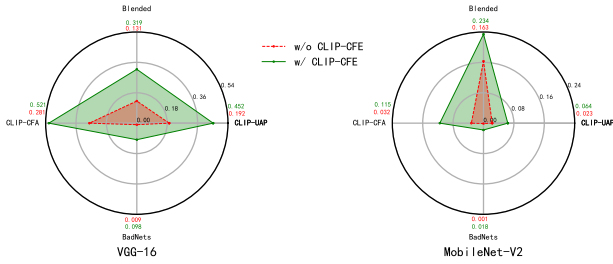


Figure 18: The attack success rate (ASR) of the class-constrained backdoor attacks (the access category  $Y'$  is set to  $\{0\}$ ) on the ImageNet-50 dataset. The red points represents w/o CLIP-based Clean Feature Erasing (CFE), while the green points represents w/ CLIP-based Clean Feature Erasing (CFE). The experiment is repeated 5 times, and the results were computed as the mean of five different runs.

accuracy under various settings and different backdoor attacks.

### 7.2.3 RQ3: Are proposed technologies effective for different poisoning settings.

**Ablation of different poison rates on the number-constrained backdoor attacks.** We conducted ablation studies to verify the effective-

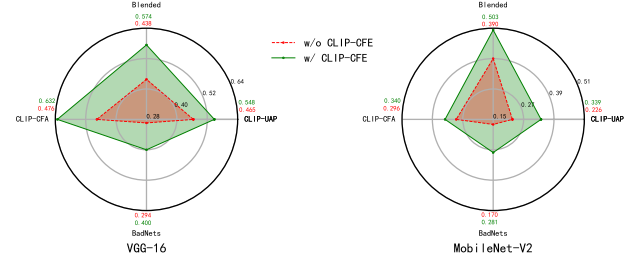


Figure 19: The attack success rate (ASR) of the class-constrained backdoor attacks (the access category  $Y'$  is set to  $\{1\}$ ) on the ImageNet-50 dataset. The red points represents w/o CLIP-based Clean Feature Erasing (CFE), while the green points represents w/ CLIP-based Clean Feature Erasing (CFE). The experiment is repeated 5 times, and the results were computed as the mean of five different runs.

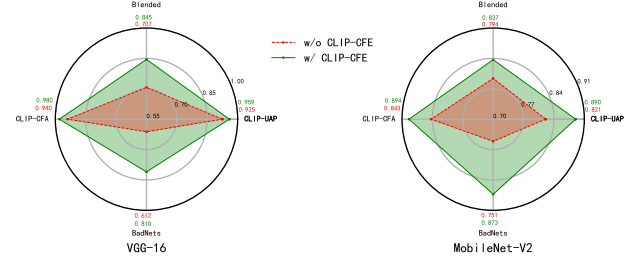


Figure 20: The attack success rate (ASR) of the domain-constrained backdoor attacks (Domain rate is set to 0) on the ImageNet-50 dataset. The red points represents w/o CLIP-based Clean Feature Erasing (CFE), while the green points represents w/ CLIP-based Clean Feature Erasing (CFE). The experiment is repeated 5 times, and the results were computed as the mean of five different runs.

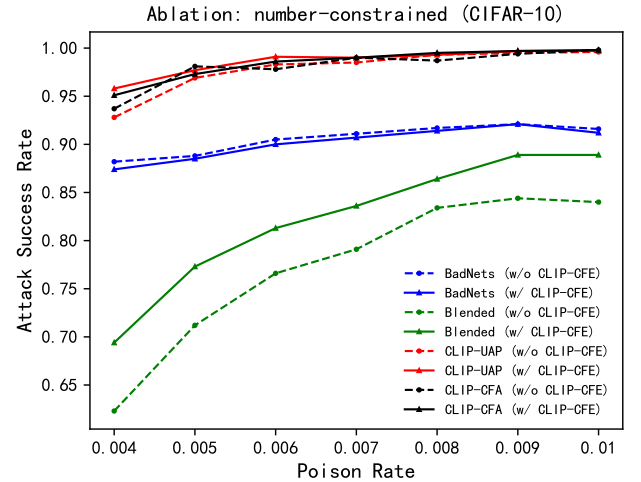


Figure 21: The attack success rate on the CIFAR-10 dataset at different poisoning rates. All results were computed as the mean of five different runs.

tiveness of the proposed methods in reducing the number of poisoning samples (poisoning rates) on the number-constrained backdoor

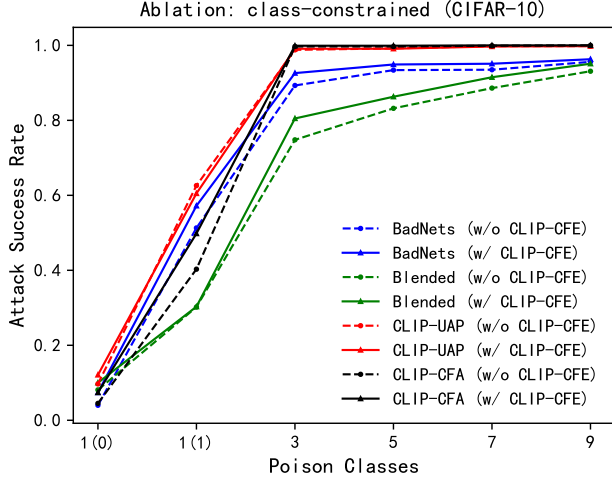


Figure 22: The attack success rate on the CIFAR-10 dataset at different accessible class of poisoning samples. All results were computed as the mean of five different runs.

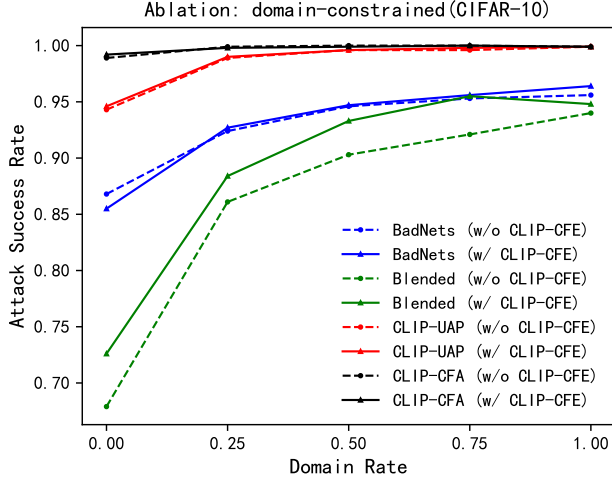


Figure 23: The attack success rate on the CIFAR-10 dataset at different proportions of in-domain samples. All results were computed as the mean of five different runs.

attacks. The results in Fig. 21 illustrate that: i) The attack success rate increases with the increase of poisoning rate for different attacks; ii) Our proposed CLIP-UAP and CLIP-CFA methods outperform the BadNets [16] and Blended [5]; iii) The proposed CLIP-CFE further improves the poisoning effectiveness upon the different triggers.

**Ablation of different poison classes on the class-constrained backdoor attacks.** In this section, we conducted ablation studies to verify the effectiveness of the proposed methods in increasing the number of poisoning classes on the class-constrained backdoor attacks. The results in Fig. 22 illustrate that: i) The attack success rate increases with the increase of poisoning classes for different attacks; ii) The attack success rate of clean-label single-class attack is lower than that of dirty-label single-class attacks; iii) Our proposed CLIP-UAP and CLIP-CFA methods outperform the BadNets [16] and Blended [5] methods; iv) The proposed CLIP-CFE method further improves the poisoning effectiveness with different triggers.

**Ablation of different domain rates on the domain-constrained backdoor attacks.** In this section, we conducted ablation studies to verify the effectiveness of the proposed methods in increasing the domain rate on the domain-constrained backdoor attacks. The results in Fig. 23 illustrate that: i) The attack success rate increases with the increase of the domain rates for different attacks; ii) Our proposed CLIP-UAP and CLIP-CFA methods outperform the BadNets [16] and Blended [5] methods; iii) The proposed CLIP-CFE method further improves the poisoning effectiveness with different triggers.

## 7.3 Experiments on the ImageNet-50 Dataset

### 7.3.1 RQ1: Are proposed technologies effective on different backdoor attacks.

In this section, we utilized our proposed technologies to attack different target models on the ImageNet-50 dataset and calculate the ASR for each target model to verify the attack effectiveness. The baseline attack methods, BadNets [16] and Blended [5] were introduced in Sec. 2.1.2. Fig. 17, 18, 19, and 20 reflect the attack performance of the number-constrained, clean-label single-class (class-constrained), dirty-label single-class (class-constrained), and out-of-the domain (domain-constrained) backdoor attacks on the ImageNet-50 dataset, respectively.

**CLIP-based Poisoning Feature Augmentation Is More Effective Than Previous Attack Methods.** Our proposed CLIP-UAP and CLIP-CFA methods outperform the BadNets [16] and Blended [5] baseline methods in terms of consistency under different attacks and datasets. This confirms that the proposed poisoning feature augmentation generates more efficient triggers than other methods. **CLIP-based Clean Feature Suppression Is Useful For Different Attack Methods.** Our proposed CLIP-CFE method improves the poisoning effectiveness on most cases compared to the baseline without CLIP-based Clean Feature Erasing. Only on the MobileNet-V2 results of the number-constrained backdoor attacks (right part of the Fig. 17), CLIP-UAP slightly outperform the corresponding methods with CFE.

### 7.3.2 RQ2: Are proposed three technologies harmless for Benign Accuracy.

Table 4 illustrates that our proposed CLIP-UAP and CLIP-CFA methods have similar or even better average Benign Accuracy (BA) compared to the baseline methods BadNets [16] and Blended [5]. Additionally, our proposed CLIP-CFE method has no negative effect on BA, confirming that our technologies are harmless for benign accuracy under various settings and different backdoor attacks.

## 7.4 Related Works

Backdoor attacks aim to introduce hidden triggers into DNNs, allowing the attacked models to behave correctly on clean samples while exhibiting malicious behavior when triggered by specific inputs. These attacks can occur at various stages of Artificial Intelligence (AI) system development [13, 27]. The surface of backdoor attacks has been systematically categorized into six groups: code-based [2, 48], outsourcing, pretrained model-based [14, 23, 56], data collection-based [5, 16, 32, 54], collaborative learning-based [40, 63], and post-deployment attacks [18, 47]. Among these categories,



poisoning-based backdoor attacks, which involve introducing a backdoor trigger during the training process by mixing a few poisoning samples, are the most straightforward and commonly used method. This study focuses on addressing concerns related to poisoning-based backdoor attacks. Furthermore, backdoor can be embedded through various techniques, such as transfer learning [14, 23, 56], controlling model parameters [4, 10, 47], adding malicious modules [28], and modifying the context of deep learning for source code [48], among others. Previous studies focusing on poisoning-based backdoor attacks typically assume that the attacker has access to the entire training set and primarily concentrate on enhancing poisoning efficiency and stealthiness.

#### 7.4.1 Poisoning Efficiency

Existing studies aim at improving the poisoning efficiency of backdoor attacks can be categorized into two main areas.

**Designing Efficient Triggers** The design of efficient triggers that are easier for DNNs to learn has garnered significant interest. Researchers have recently drawn inspiration from Universal Adversarial Perturbations (UAPs) [38] and optimized UAPs on pre-trained clean models to create effective triggers, which have been widely utilized in various studies [9, 26, 70]. However, this approach requires a pre-trained clean model on the training set, which is not practical for data-constrained backdoor attacks.

**Selecting Efficient Poisoning Samples** Efficient sample selection for poisoning attacks is a critical yet under-explored aspect that is distinct from trigger design. Xia *et al.* [60] were among the first to investigate the contribution of different data to backdoor injection. Their research revealed that not all poisoning samples contribute equally, and appropriate sample selection can greatly enhance the efficiency of data in backdoor attacks.

#### 7.4.2 Poisoning Stealthiness

Existing studies focused on increasing the stealthiness of backdoor attacks can be categorized into two main areas.

**Designing Invisible Triggers** The concept of invisible triggers aims to ensure that poisoning images are visually indistinguishable from clean samples, thus evading detection in both pixel and feature spaces. This perspective is the most straightforward approach to bypass defenses. Chen *et al.* [5] first propose a blended strategy to evade human detection by blending clean samples with the trigger to create poisoning samples. Subsequent studies [9, 26, 70] focus on constraining the norm of the trigger through optimization methods. Moreover, some studies have explored the use of natural patterns such as warping [39], rotation [59], style transfer [7], frequency [12, 66], and reflection [35] to create triggers that are more imperceptible to human inspection. In contrast to previous works that employ universal triggers, Li *et al.* [29] employ GAN models to generate sample-specific triggers, which are similar to adversarial examples and extremely imperceptible to humans.

**Clean-label Attacks.** Clean-label attacks refer to backdoor attacks where the target labels of the poisoning samples align with their perception labels. Turner *et al.* [54] is the first to explore clean-label attacks by employing GAN-based and adversarial-based perturbations. Compared to standard backdoor attacks, clean-label attacks are typically less effective due to the model’s tendency to associate natural features, rather than backdoor triggers, with the tar-

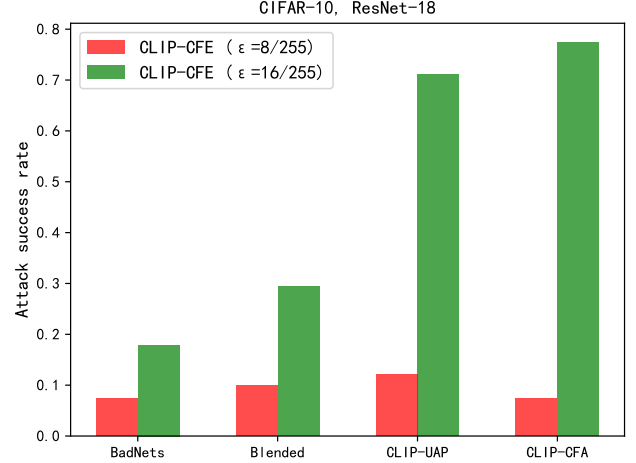


Figure 24: The attack success rate on the CIFAR-10 dataset at different  $\epsilon$ . All results are computed as the mean of five different runs.

get class. Recent studies have focused on aligning features [50] or gradients [53] between perturbed inputs from the target class and trigger-inserted inputs from the non-target class through pretraining on the entire training set. Additionally, some study [65] has proposed optimizing the backdoor trigger using only the knowledge about the target-class training data. In this approach, the trigger is optimized to point towards the interior of the target class, resulting in improved effectiveness.

## 7.5 Discussion

**Performance degradation in the clean-label single-class backdoor attack.** As depicted in Fig. 7 (b), Fig. 14, and Fig. 18, both the baseline and our attack methods exhibit poor Attack Success Rate (ASR) in the clean-label single-class backdoor attack. In this section, we aim to enhance the attack strength of our methods and devise a more efficient attack strategy for the clean-label single-class backdoor attack. In our optimization equations, namely Eq. 4, Eq. 9, and Eq. 13, we impose constraints on the optimized noise, denoted as  $\delta_i$ ,  $\delta_{uap}$ , and  $\delta_{con}$ , respectively. These constraints are specified as  $\|\delta_i\|_p \leq \epsilon$ ,  $\|\delta_{uap}\|_p \leq \epsilon$ , and  $\|\delta_{con}\|_p \leq \epsilon$ , where  $\|\cdot\|_p$  represents the  $L_p$  norm, and we set  $\epsilon$  to  $8/255$  to ensure the stealthiness of the backdoor attacks, as observed in our previous experiments. To bolster the attack strength and subsequently increase the ASR in the clean-label single-class backdoor attack, we investigate the impact of adjusting the constraint on  $\delta_i$ . As demonstrated in Fig. 24 and Fig. 25, significant (more than 500%) improvements are observed in the ASR of the clean-label single-class backdoor attack when we set the constraint on  $\delta_i$  to  $\|\delta_i\|_p \leq 16/255$ . This finding validates the efficacy of our method in the clean-label single-class backdoor attack, albeit at the expense of compromising stealthiness. This sacrifice, which is common in previous backdoor attack methods [65], is a low-cost trade-off.

**Domain-constrained backdoor attacks are easier than class-constrained backdoor attacks.** Fig. 26 provides a visualization of the Attack Success Rate (ASR) achieved by different attack methods on the CIFAR-10 dataset in domain-constrained (domain rate set to 0) and dirty-label single-class backdoor attacks. While domain-

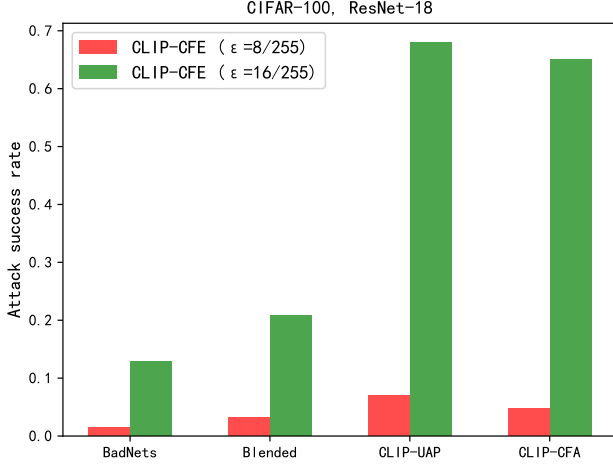


Figure 25: The attack success rate on the CIFAR-100 dataset at different  $\epsilon$ . All results are computed as the mean of five different runs.

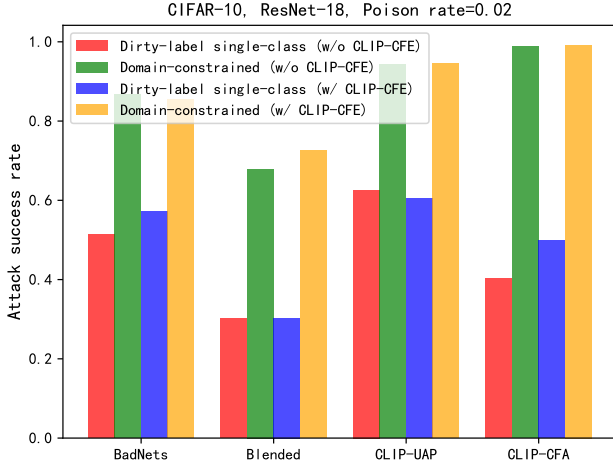


Figure 26: The attack success rate on the CIFAR-10 dataset at domain-constrained (domain rate is set to 0) and dirty-label single-class backdoor attacks. poisoning rate is set to 0.02 and all results are computed as the mean of five different runs.

constrained backdoor attacks impose stricter restrictions (assumptions that attackers have no access to any data in the training set), the ASR in domain-constrained backdoor attacks consistently surpasses that of dirty-label single-class backdoor attacks. This observation leads us to propose that the diversity of samples in the poisoning set is another crucial factor affecting attack efficiency. Consequently, we recommend that attackers fully consider the diversity of poisoning samples during the poisoning set generation phase.

## Availability

All codes and datasets will be publicly available.